

1 **BREEDIT: A novel multiplex genome editing strategy to improve complex**
2 **quantitative traits in maize (*Zea mays* L.)**

3 Christian Damian Lorenzo,^{1,2} Kevin Debray,^{1,2} Denia Herwegh,^{1,2} Ward Develtere,^{1,2} Lennert
4 Impens,^{1,2} Dries Schaumont,³ Wout Vandeputte,^{1,2} Stijn Aesaert,^{1,2} Griet Coussens,^{1,2} Yara de
5 Boe,^{1,2} Kirin Demuynck,^{1,2} Tom Van Hautegeem,^{1,2} Laurens Pauwels,^{1,2} Thomas B. Jacobs,^{1,2} Tom
6 Ruttink,³ Hilde Nelissen,^{1,2} and Dirk Inzé^{1,2,*},[†]

7
8 ¹Center for Plant Systems Biology, VIB, B-9052 Gent, Belgium

9 ²Department of Plant Biotechnology and Bioinformatics, Ghent University, B-9052 Gent, Belgium

10 ³Flanders Research Institute for Agriculture, Fisheries and food (ILVO), B-9820 Merelbeke,
11 Belgium

12

13 * Author for correspondence: dirk.inze@psb.ugent.be

14 [†] Senior author

15 These authors contributed equally (C.D.L., K.D.).

16 C.D.L. extracted DNA samples, designed and performed the phenotypical experiments,
17 performed crosses and generated the plant material after T1 generation. K.D. analyzed the data
18 and created the visualizations. C.D.L., K.D. and D.I. drafted the manuscript. T.V.H., H.N., D.H.
19 and D.I. selected the candidate genes. W.D., D.H. and T.B.J. designed gRNAs and primers. T.R.
20 curated gene models and initiated the HiPlex sequencing. W.D. and T.B.J. designed, constructed
21 and cloned the SCRIPTs. L.I. and L.P. transformed B104 inbred line to create the EDITOR and
22 SCRIPT lines.

23 D.S., K.D., and T.R. created bioinformatics pipelines to process and analyze HiPlex sequencing
24 reads. S.A. and G.C. performed the plant transformations, performed initial plant crosses and
25 generated plant material for T0-T1 generation. W.V., Y.B., K.D. assisted with phenotyping, DNA
26 extractions and greenhouse organization. H.N., T.B.J., T.R., L.P. and D.I. initiated and supervised
27 the project.

28 The author responsible for distribution of materials integral to the findings presented in this article
29 in accordance with the policy described in the Instructions for Author
30 (<https://academic.oup.com/plcell>) is: Dirk Inzé (dirk.inze@psb.vib-ugent.be).

31

32 **ORCID IDs:** 0000-0003-3954-0234 (C.D.L.); 0000-0003-2898-9415 (K.D.); 0000-0001-7744-
33 6375 (D.H.); 0000-0002-7171-8031 (W.D.); 0000-0002-6330-4744 (L.I.); 0000-0002-4389-0440
34 (D.S.); 0000-0001-7813-3645 (W.V.); 0000-0001-8787-7347 (S.A.); 0000-0003-2285-5782
35 (G.C.); 0000-0003-3079-2865 (Y.D.B.); 0000-0002-8772-3505 (K.D.); 0000-0003-3173-2477
36 (T.V.H.); 0000-0002-0221-9052 (L.P.); 0000-0002-5408-492X (T.B.J.); 0000-0002-1012-9399
37 (T.R.); 0000-0001-7494-1290 (H.N.); 0000-0002-3217-8407 (D.I.)

38 **SHORT TITLE:** BREEDIT: A novel multiplex genome editing strategy

39 **CORRESPONDING AUTHOR:**

40 Dirk Inzé

41 Center for Plant Systems Biology

42 VIB-Ghent University

43 Technologiepark 71, B-9052 Gent (Belgium).

44 Tel.: +32 9 3313800; Fax: +32 9 3313809; E-mail: dirk.inze@psb.vib-ugent.be

45

46 **Abstract**

47 Ensuring food security for an ever-growing global population while adapting to climate change is
48 the main challenge for agriculture in the 21st century. Though new technologies are being applied
49 to tackle the problem, we are approaching a plateau in crop improvement using conventional
50 breeding. Recent advances in gene engineering via the CRISPR/Cas technology pave the way to
51 accelerate plant breeding and meet this increasing demand. Here, we present a gene discovery
52 pipeline named ‘BREEDIT’ that combines multiplex genome editing of whole gene families with
53 crossing schemes to improve complex traits such as yield and drought resistance. We induced
54 gene knockouts in 48 growth-related genes using CRISPR/Cas9 and generated a collection of
55 over 1000 gene-edited maize plants. Edited populations displayed, on average, significant
56 increases of 5 to 10% for leaf length and up to 20% for leaf width compared with controls. For
57 each gene family, edits in subsets of genes could be associated with increased traits, allowing us
58 to reduce the gene space needed to focus on for trait improvement. We propose BREEDIT as a
59 gene discovery pipeline which can be rapidly applied to generate a diverse collection of mutants
60 to identify subsets of promising candidates that could be later incorporated in breeding programs.

61

62 **Keywords**

63 Multiplex gene editing; CRISPR/Cas9; multiplex amplicon sequencing; maize; gene family;
64 network engineering; reverse genetics

65

66 **Introduction**

67 The production of enough food to feed the increasing global population is facing many
68 challenges due to climate change. Extreme temperature ranges, reduction of water availability
69 and limited use of arable land are all expected to converge on a significant drop in crop yields
70 (Zhang and Cai, 2011; Long et al., 2015; Brás et al., 2021). During the past century, conventional
71 breeding has been decisive to adapt crops to local environments and to increase yield under stress
72 conditions (Nuccio et al., 2018; Snowdon et al., 2021). Genomics-assisted breeding has greatly
73 contributed to generate new varieties by incorporating haplotype information in breeding
74 programs (Bhat et al., 2021). Nonetheless, we are slowly approaching a plateau in crop

75 improvement using conventional breeding, since gene discovery and introgression of favorable
76 alleles cannot be implemented fast enough to cope with the losses caused by environmental
77 stresses.

78 In that perspective, innovative strategies need to be implemented to bridge the gap
79 between conventional breeding and the knowledge acquired through plant molecular biology to
80 further improve complex traits such as yield. Crop yield is determined by the complex interaction
81 of the (a)biotic environment with the genetically determined growth and developmental processes
82 that drive the plant's life cycle (Elias et al., 2016). There are numerous yield-related traits such as
83 early seedling vigor, root and shoot architecture, biomass allocation, resource use efficiency,
84 senescence, seed filling, etc. In some cases, such as disease resistance, few causative genes
85 control the expression of the trait. However, for many yield- and growth-related quantitative traits
86 (e.g. organ growth, tolerance to abiotic stress such as drought), numerous, small-effect genes
87 contribute (Mickelbart et al., 2015; Poland and Rutkoski, 2016). Traditionally, yield
88 improvement has been tackled from two distinct angles. Breeding aims at producing genetic
89 combinations with better performance, whereas molecular biology works to understand the mode
90 of action of yield-related genes. These two fields operate at very different scales; breeding
91 recombines chromosomal segments towards a favorable genome constitution, whereas molecular
92 biology only deals with a limited number of genes. In crop breeding programs, phenotypes (e.g.
93 seed yield) are collected from many individuals and multi-year/multi-location field trials. By
94 correlating the phenotypes with the genotypic diversity of individuals, genetic variants associated
95 with the improved trait values can be identified (Rasheed et al., 2017). Using this approach, many
96 quantitative agronomic traits have been found to be determined by numerous small-effect loci,
97 with the underlying genomic regions known as 'quantitative trait loci' or QTLs. Such QTLs are
98 generally searched for in segregating mapping populations of recombinant inbred lines (RILs)
99 obtained from two or more parents. A more recent variant of this approach is the genome-wide
100 association study (GWAS), in which numerous genome-wide markers are assayed in many
101 diverse genotypes to associate loci with the phenotypic trait (Wang and Qin, 2017). Furthermore,
102 the combination of phenotypic trait data with the availability of a high number of genomic
103 markers, or even the entire genome sequence, can be used for genomic prediction to increase the
104 predictability of the breeding value of new material (Voss-Fels and Snowdon, 2016). Although
105 these marker-assisted breeding technologies have a major impact on the accuracy and speed of

106 crop breeding, the genes underlying the QTLs are in many cases unknown. In recent years,
107 technological advances have combined GWAS with molecular -omics phenotypes that go beyond
108 the genomic information, so that molecular networks start to emerge in molecular breeding
109 (Baute et al., 2015; Baute et al., 2016; Xiao et al., 2016; Miculan et al., 2021).

110 Over the past four decades, there has been tremendous progress in the understanding of
111 the molecular basis of many different plant processes. The use of model organisms such as
112 *Arabidopsis* and rice has been a driving force. A vast amount of research delivered insights into
113 the molecular pathways steering seed development, root growth, leaf development, plant
114 architecture, tolerance to severe drought stress, cold tolerance, flooding and many more
115 agronomic traits. Combined, this information reinforced the idea that plant growth and possibly
116 crop yield may be improved by altering the expression of specific (regulatory) genes. Indeed,
117 many reports have shown that positive effects of yield-related traits could be obtained by
118 modifying the expression of individual genes. In *Arabidopsis*, more than 60 genes were identified
119 that, when ectopically expressed or down-regulated, increase leaf size and in many cases also the
120 size of other organs, including seeds (for reviews, see Gonzalez et al., 2012; Czesnick and
121 Lenhard, 2015; Vercruyssen et al., 2020). Likewise, numerous genes that can be used to improve
122 seed yield and size in rice have been identified (Li and Li, 2016). Based on these observations,
123 agro-biotech companies have initiated large-scale programs in the beginning of the 21st century to
124 investigate the effect of numerous selected genes on agronomic traits in crops of interest, mainly
125 maize and rice. The conclusion of these studies was that although positive effects were often
126 noticed in the greenhouse and even in field trials, the observed changes were often too small and
127 too much dependent on the genotype and the environment to justify further investments in
128 pursuing this high-throughput screening approach (Paul et al., 2018; Simmons et al., 2021). Why
129 is it so challenging to translate basic insights in molecular networks and genes into improved
130 crops? In breeding, the phenomenon of expressivity is well-known. Expressivity measures the
131 extent to which a given genotype is expressed at the phenotypic level. The concept of
132 expressivity is best explained by the notion that genes often work in complex networks with
133 many different levels of regulation. Such higher-order regulation is typically exerted on complex
134 and essential processes, such as growth, that need to integrate a panoply of endogenous,
135 genetically determined signals as well as environmental cues. Single-point perturbations of
136 networks often have a limited effect because other components of the network take over to buffer

137 the system. However, in many cases, the combination of perturbations of a network makes
138 phenotypes much more visible. For example, the pairwise combinations of 13 *Arabidopsis*
139 growth-related genes (GRGs), each enhancing leaf size on their own when ectopically expressed
140 or mutated, lead in more than 80% of the combinations to additive or synergistic effects on leaf
141 size (Vanhaeren et al., 2014; Vanhaeren et al., 2017). Moreover, a triple combination of three
142 different mutants of GRGs increased the size of leaves, flowers, seeds and even roots of
143 *Arabidopsis* in a spectacular manner (Vanhaeren et al., 2017). Also in maize, albeit with fewer
144 genes, pairwise combinations of specific alleles of growth-enhancing genes result in additive
145 effects (Sun et al., 2017; Liu et al., 2021). This concept is also clearly observed during breeding,
146 when yield traits most often are determined by many small-effect loci that need to work in
147 concert to obtain a maximal output.

148 Despite the spectacular advances made by systems biology in integrating large data sets,
149 the mechanisms behind the control of plant developmental processes are so complex that
150 predicting which combination of genes would provide the optimal effect on yield remains
151 virtually impossible. Understanding the mode of action might be the best way forward to estimate
152 the combinability of genes (Vanhaeren et al., 2014; Sun et al., 2017). However, even when
153 dealing with a relatively small number of genes, testing all possible pairwise gene combinations
154 remains cumbersome and resource intensive. The investments become even more important when
155 triple or higher-order gene combinations have to be tested, which is necessary to achieve stable
156 yield increases of 10% or higher.

157 The clustered regularly interspaced short palindromic repeat (CRISPR) technology
158 emerged as a powerful tool for simultaneously multiplex-targeting several GRGs, easily
159 generating genetic variability in a broad set of targets and thus enabling a plethora of
160 combinatorial mutations to be analyzed (Knott and Doudna, 2018; Zhang et al., 2019). Several
161 studies showed how CRISPR could be used to reshape plant architecture and target complex
162 traits in multiple species like tomato (Rodríguez-Leal et al., 2017; Wang et al., 2021), wheat (Li
163 et al., 2020), rice (Meng et al., 2017) and in maize (Doll et al., 2019). As a broader application,
164 large-scale CRISPR screens have been carried out in rice (Lu et al., 2017), cotton (Ramadan et
165 al., 2021), maize (Liu et al., 2020; Gong et al., 2022), tomato (Jacobs et al., 2017), oilseed rape
166 (Li et al., 2018) and soybean (Bai et al., 2020).

167 Here, we explored an experimental approach to bridge the gap between conventional
168 breeding and genetic engineering of multiple genes by combining multiplex CRISPR-mediated
169 genome editing with crossing schemes to observe favorable phenotypes. We denominated this
170 approach BREEDIT, a contraction of breeding and gene editing, and propose this strategy as a
171 powerful technique to engineer complex traits by knocking out a large number of key players in
172 gene families and pathways. In just two generations, we generated a list of putative gene
173 knockouts (KOs) required to evoke clear yield-related phenotypes in maize. BREEDIT could
174 therefore be used to rapidly identify a subset of genes involved in the expression of a complex
175 trait and identify targets for plant breeding programs.

176

177 **Results**

178 **Development of a CRISPR/Cas9 multiplex genome editing pipeline in maize: general** 179 **outline**

180 The aim of this study was to develop a flexible pipeline that combines multiplex gene editing and
181 different crossing schemes to generate plants with modified traits (Figure 1). First, 48 candidate
182 GRGs (Table 1) were selected based on the literature or in-house knowledge, in the target species
183 maize, complemented with other model organisms, i.e. *Arabidopsis* and rice (Figure 1A). For
184 instance, negative growth regulators whose inactivation is likely to result in positive effects on
185 growth are suitable GRG candidates. Guide RNAs (gRNAs) targeting these GRGs are designed
186 and cloned into multiplex gene editing vectors (referred to as SCRIPTs), which are then used to
187 transform *Cas9*-expressing lines (named EDITOR lines), resulting in super transformed lines that
188 harbor both *Cas9* and a SCRIPT containing 12 gRNAs (Figure 1B; Supplemental Figure S1). The
189 BREEDIT pipeline then uses highly multiplex (HiPlex) amplicon sequencing combined with the
190 SMAP haplotype-window bioinformatics workflow to routinely monitor gene edits at gRNA
191 cutting sites. Amplicon sequencing at great depths enables to collect haplotype sequences and
192 their respective frequencies (Figure 1D). Both types of information can be used to assess the
193 effect of mutations on the encoded protein function or activity and assign a genotype to the plant
194 for a specific locus. Per sample and per locus, the length difference between a mutated haplotype
195 and the reference haplotype is used to classify the mutated haplotypes in two categories:
196 haplotype_{KO} corresponds to haplotypes containing out-frame insertions or deletions (indels),
197 leading to a gene KO and an nonfunctional protein; haplotype_{REF} includes haplotypes with only

198 single-nucleotide polymorphisms (SNPs) outside the cutting site or in-frame indels supposed to
199 have less impact on the translated protein that may still behave as the reference protein. In
200 CRISPR/Cas9 experiments, one plant may contain more haplotypes than its ploidy level because
201 of mosaic tissues as a consequence of the initial (T0) or ongoing (T1, T2) Cas9 activity, thus
202 complicating the genotyping. To interpret complex haplotype constitutions, the relative fraction
203 of all haplotype_{KO} is summed per locus per sample. The resulting aggregation is interpreted as a
204 gene loss-of-function (LOF) dosage, further discretized in three categories: LOF_{0/2} (none of the
205 two chromosomes is affected by a set of haplotype_{KO}), LOF_{1/2} (one of the two chromosomes is
206 affected by a set of haplotype_{KO}), and LOF_{2/2} (both chromosomes are affected by a set of
207 haplotype_{KO}). The three dosage categories are used in genotype-to-phenotype associations.

208 After selecting transgenic lines, T0 lines are genotyped and the T0 plants with the highest
209 numbers of gene KOs (either partial (LOF_{1/2}) or complete (LOF_{2/2})) are crossed to obtain material
210 for phenotyping (Figure 1C). Different crosses can be performed to maximize the number of
211 edited genes as well as to fix combinations of gene edits. Self-crosses serve to fix edits in parallel
212 to maximize phenotypic readout, while backcrosses to the original line provide heterozygous
213 lines which can later be self-crossed and phenotyped in T2. Additional specific crosses can be
214 performed to further enrich edit diversity. Plants harboring the same SCRIPT but containing edits
215 at different genes from that SCRIPT can be crossed to increase the number of gene edits (up to
216 12) in the corresponding gene family or pathway. Such crosses will be further referred to as intra-
217 script crosses. Furthermore, plants transformed with different SCRIPTs can be crossed to
218 maximally combine mutants in genes covered by different families or pathways. These crosses
219 will be further referred to as inter-script crosses. Since Cas9 remains active in all subsequent
220 generations (Impens et al., 2022), new transgenerational edits are expected to accumulate,
221 resulting in a large collection of higher-order mutants (up to 24 gene edits when two SCRIPTs
222 are combined) in different segregating states (i.e. LOF_{0/2}, LOF_{1/2} or LOF_{2/2}).

223 Because several plants are generated following the BREEDIT approach, easy-to-measure
224 quantitative traits are used to maximize the throughput of the phenotyping steps. Despite the high
225 number of plants generated, each individual has likely a unique genotypic profile given the many
226 combinations of indels and dosage that can happen in a set of 12 genes or more. Therefore,
227 repetitions of same genotypic combinations cannot be used for statistics in BREEDIT. The
228 effects of combinations of gene edits on traits are better appraised at the population level, though

229 the specific causative gene combination cannot be deduced. The effect of a single gene on a trait
230 can however still be evaluated considering that multiple observations of a single gene KO would
231 conceal the putative noise brought by mutations in other genes. The framework for phenotyping
232 experiments consists of several (minimum two) independent trials to test the performance of
233 independent mutated populations compared with the EDITOR line. Single-gene associations to a
234 trait are then conducted per experiment per population. The number of times a gene KO is
235 significantly associated with a trait across different independent populations and experiments is a
236 measure for the importance of that gene in the expression of the trait. At the end of the BREEDIT
237 pipeline, genes can be ranked to delineate a minimal set of candidate genes with maximal effect
238 on trait expression, thus reducing the gene space to be considered for further research.

239

240 **Applying the BREEDIT strategy**

241 To test the BREEDIT strategy, we selected 48 maize GRGs with potential positive effects on
242 growth when mutated, individually or in combination (Table 1). The gRNAs targeting the 48
243 genes were distributed over SCRIPT 1 to SCRIPT 4 and were, as much as possible, grouped per
244 gene family. This distribution primarily aims to simultaneously knockout multiple members of
245 the same gene family/pathway to overcome potential functional redundancy of paralogs. In
246 addition, grouping by family aims to generate segregating mutants with a range of gene KOs,
247 which may help to untangle complex relationships in gene regulatory networks that might be
248 overlooked when only single or double mutants are considered. Additionally, chromosomal
249 positions of the GRGs were taken into consideration to spread the distribution of genes belonging
250 to a same SCRIPT over chromosomes when possible (Supplemental Figure S2). The 12 genes
251 targeted in SCRIPT 1 are major players in gibberellin catabolism and signaling. The 12 genes
252 targeted in SCRIPT 2 are maize orthologs of genes encoding cytokinin oxidases (*CKXs*), key
253 regulators of cytokinin catabolism. SCRIPT 3 contains gRNAs for eight genes encoding the
254 family of inhibitors of cyclin-dependent kinase/Kip-related proteins (*ICK/KRP*), as well as four
255 genes expected to encode negative regulators of growth under drought conditions: two maize
256 *PP2C* orthologs (*ZmPP2Cs*) and two *HOMEODOMAIN*-type genes (*HB124B* and *HB124C*),
257 orthologs of the *Arabidopsis* genes *PHABULOSA* and *PHAVOLUTA* (McConnell et al., 2001).
258 Finally, SCRIPT 4 contains gRNAs for seven orthologs of class II *CINCINNATA-TEOSINTE*
259 *BRANCHED 1/CYCLOIDEA/PROLIFERATING CELL FACTOR* (*CIN-TCP*) and three members

260 of the *GROWTH REGULATING FACTORS (GRF)* genes, major regulators of cell division, leaf
261 shape and leaf size determination. Additionally, gRNAs targeting an ortholog of the GAGA-
262 binding protein-encoding *BASIC PENTACYSTEINE 6 (ZmBPC6)* and a gene encoding a plant
263 homeodomain (PHD)-finger protein (*ZmPHD8*) were included in SCRIPT 4.

264

265 **Generation of highly edited maize populations for all SCRIPTs**

266 We developed a set of three independent homozygous EDITOR lines that constitutively express
267 the Cas9 protein in the maize inbred line B104 (Supplemental Figure S3) to execute editing at
268 loci targeted by arrays of 12 gRNAs expressed from the SCRIPT vector. EDITOR 1 and
269 EDITOR 3 were supertransformed with SCRIPT 1 for a preliminary evaluation of gene editing.
270 After transformation, the EDITOR 1 and EDITOR 3 supertransformed populations showed
271 similar editing profiles (Supplemental Figure S4). At T0, six out of the 12 targeted genes showed
272 LOF_{1/2} or LOF_{2/2} in both EDITOR lines and the number of mutant alleles at each locus was
273 comparable between both EDITOR backgrounds. The same gRNAs were active in both EDITOR
274 backgrounds but four genes out of the six being commonly edited in both EDITOR backgrounds
275 have LOF_{2/2} in EDITOR 1 whereas two in EDITOR 3 (Supplemental Figure S4). We proceeded
276 with EDITOR 1 as the genetic background for further experiments and supertransformed this line
277 with the remaining three scripts. Like for SCRIPT 1, we monitored gene edits in T0 plants and all
278 subsequent generations using HiPlex amplicon sequencing. Indels in haplotype sequences ranged
279 from -90 bp to +92 bp. Insertions of one nucleotide (+1 bp) were the most represented type of
280 mutation, but overall, deletions were more present than insertions (Figure 2A). The largest
281 insertions showed sequence similarity to genomic fragments located up to 1 kb upstream or
282 downstream of the expected cutting site. At T0, we detected haplotype_{KO} in 11, 12, 8, and 12 out
283 of the 12 target sites for SCRIPT 1, 2, 3, and 4, respectively (Figure 2B). Across all T0 SCRIPT
284 populations, a large diversity of haplotypes (109 haplotypes with in-frame and 407 haplotypes
285 with out-frame indels) could be identified (Supplemental Figure S5). Some haplotype_{KO} were
286 initially not detected at T0, but appeared in T1 populations (Figure 2B) of both intra-script and
287 inter-script crosses, revealing either ongoing gene editing in subsequent generations or
288 overlooked edits due to mosaic tissues in T0. Overall, from T0 to T2, mutations could be found in
289 all the 48 targeted genes, except one (*SPY* in SCRIPT 1). We focused on haplotype_{KO}, and
290 observed a diversity of haplotype_{KO} combinations per locus per sample (mono-, bi-, multi-allelic)

291 in the T0 to T2 samples, all expected to lead to a gene LOF, either partial ($\text{LOF}_{1/2}$) or complete
292 ($\text{LOF}_{2/2}$) (Figure 2C). We observed a typical tri-modal distribution for the aggregated fraction of
293 haplotype_{KO} that could be roughly divided into three areas with higher counts, each
294 corresponding to a discrete genotypic class ($\text{LOF}_{0/2}$, $\text{LOF}_{1/2}$, and $\text{LOF}_{2/2}$; Supplemental
295 Figure S6).

296

297

298 **From haplotype frequencies to genotypic information**

299 The aggregated fraction of haplotype_{KO} in sequencing reads was used as a proxy to characterize
300 partial ($\text{LOF}_{1/2}$) and complete ($\text{LOF}_{2/2}$) gene KOs (Figure 3). Our approach for the detection of
301 gene edits using HiPlex amplicon sequencing combined with SMAP haplotype-window analyses
302 successfully captured haplotype sequences in 96% of the cases, encouraging us to use this
303 technique to monitor edits in the offspring (Figure 3A). At T0, 73% (35/48) of the target loci
304 showed $\text{LOF}_{1/2}$ or $\text{LOF}_{2/2}$, with SCRIPT 1 and SCRIPT 3 performing less than SCRIPT 2 and
305 SCRIPT 4 (Figure 3B). At T1, of the 13 remaining genes not edited at T0, 12 (92%) were *de*
306 *novo* edited. No haplotype_{KO} was observed at the last remaining non-edited locus (*SPY*) at T2.
307 Also, all the transgenerational *de novo* edits were only heterozygous mono-allelic mutations
308 (Figure 3B). Considering both T0 and T1 materials, we observed plants stacking up to nine
309 $\text{LOF}_{1/2}$ or $\text{LOF}_{2/2}$ in both SCRIPT 1 and SCRIPT 3, and 11 of $\text{LOF}_{1/2}$ or $\text{LOF}_{2/2}$ gene KOs in
310 SCRIPT 2 and SCRIPT 4 (Figure 3C). Because of sterility issues, progeny of SCRIPT 1 was
311 difficult to generate by crossing, resulting in the low numbers of T2 for that SCRIPT (Figure 3C).
312 Finally, we also studied progeny resulting from inter-script crosses involving two SCRIPTs ($2 \times$
313 12 target loci) and observed that, on average, 40% of the loci showing edits in the progeny
314 presented transgenerational editing patterns and 25% were completely *de novo* edited, meaning
315 that edits at these loci were not observed in the parental lines (Supplemental Figure S7). Per locus
316 across all populations, on average 7% of the progeny is affected by transgenerational edits
317 inducing $\text{LOF}_{1/2}$ at the target sites.

318 In conclusion, the approach of supertransforming EDITOR lines with SCRIPT constructs
319 generated a high frequency of heritable edits in T0 and additional transgenerational edits in T1
320 and T2.

321

322 **T1 single-SCRIPT multiple-edited populations display phenotypic variability in seedling**
323 **growth-related traits**

324 After we generated the single-SCRIPT populations of edited plants, we studied the effects of
325 multiple gene edits on plant growth by phenotyping T1 maize seedlings derived from T0 selfings
326 of each SCRIPT at the V3 stage. To facilitate high-throughput phenotyping of several
327 populations, we scored easy-to-measure parameters such as the final leaf length and width of leaf
328 3 (FLL3 and FLW3, respectively) and also integrative parameters such as the fresh weight (FW),
329 dry weight (DW) and moisture content of plants grown under well-watered (WW) and water-
330 deficient (WD) conditions. We scored populations derived from independent transgenic events to
331 analyze the effect of combinations of LOF dosages resulting from different haplotype_{KO} on trait
332 expression (Figure 4, gradient of edits displayed in orange). Detailed information of the different
333 populations that were phenotyped is provided in Supplemental Table S1.

334 SCRIPT 1 plants were tested in two independent WW experiments (WW001 and
335 WW008) (Figure 4A, B) and displayed conspicuous phenotypes such as a slender shoot
336 architecture (Figure 4C) with longer and narrower leaves (Figure 4A-B, E) compared with
337 EDITOR 1 controls. The most conspicuous phenotypes could be observed in population P013,
338 which includes individuals with partial or complete LOF in a set of 11/12 genes (Figure 4A-E).
339 Additionally, some SCRIPT 1 plants displayed abnormal tassel development with a lack of
340 florets or pollen and the formation of silks in the anthers (Supplemental Figure S8), leading to
341 male sterility.

342 For SCRIPT 2 and SCRIPT 3, when tested in experiment WW001, significant increases
343 of about 5% relative to controls could be detected only for FLL3 and only in one of the two
344 populations of each group (P108 for SCRIPT 2, and P033 for SCRIPT 3), while FLW3 remained
345 unaffected in SCRIPT 2 populations or decreased for both populations of SCRIPT 3
346 (Supplemental Figure S9B-C). Because the genes targeted in SCRIPT 2 are involved in cytokinin
347 metabolism, previously implicated in drought tolerance (Rida et al., 2021), and some of the genes
348 targeted in SCRIPT 3 are drought responsive (Li et al., 2016; Hai et al., 2020), these populations
349 were phenotyped under WD conditions (Supplemental Figure S9B-C). Under WD, the SCRIPT 2
350 populations showed an enhanced growth (Supplemental Figure S10A), which is reflected by a
351 significant increase in FLL3, FLW3, FW and DW compared with control EDITOR 1
352 (Supplemental Figure S9B, Supplemental Figure S10 A-C). For SCRIPT 3, all tested populations

353 displayed enhanced growth traits (Supplemental Figure S11), but only significant increases in
354 FLL3 compared with EDITOR 1 were observed (Supplemental Figure S9C). Moreover,
355 population P034 presented a significant increase for FW compared with EDITOR 1 controls
356 (Supplemental Figures S9C and S11).

357 Changes in leaf morphology were also observed for SCRIPT 4 plants (TCP, GRF family
358 genes). Individuals that segregate LOF dosages in 12/12 and 9/12 genes were observed in
359 populations P059 and P060, respectively (Figure 4F-G, gradient of edits in orange; Supplemental
360 Table S1). Both populations presented significantly longer FLL3 (Figure 4F) alongside a >15%
361 increase in FLW3 compared with EDITOR 1 (Figure 4G-I). The increase in FLL3 could not be
362 detected in populations P054, P079, and P130 (Figure 4F, Supplemental Table S1) but the rise in
363 FLW3 was significantly detected in all populations (Figure 4G).

364

365 **Crossing plants with different SCRIPTs allows combining phenotypes in T2 plants**

366 After focusing on single-SCRIPT populations, we phenotyped inter-script populations that stack
367 edits in genes from different SCRIPTs after crossings. For this, T0 plants with different scripts
368 were crossed and the resulting T1 plants (inter-script crosses) were self-crossed. Of all the
369 different combinations, we phenotyped two T2 inter-script populations which presented different
370 profiles of edits in crosses between SCRIPT 2 × SCRIPT 4 (P148 and P152) and SCRIPT 3 ×
371 SCRIPT 4 (P157 and P158) under WD conditions. For both populations of SCRIPT 2 ×
372 SCRIPT 4 and SCRIPT 3 × SCRIPT 4, we detected a significant increase in FLW3
373 (Supplemental Figure S12, and Supplemental Table S1), a phenotype observed in single-
374 SCRIPT 4 T1 lines. For the other traits, distinct differences were observed in each population.
375 P148 displayed an increase in FLL3, whereas P152 showed a decrease in FLL3 and significant
376 increases in FW and moisture content compared with the EDITOR 1 control (Supplemental
377 Figure 12A). Both P157 and P158 displayed significant increases in moisture content and P158
378 displayed reduced DW compared with the EDITOR 1 control (Supplemental Figure 12B).

379

380 **Genotype-to-phenotype associations and gene space reduction**

381 After phenotypic evaluation of all SCRIPT populations, we attempted to determine the possible
382 causative genes for the observed phenotypes. Because each individual phenotyping experiment

383 did not allow for sufficient replication of LOF dosages combinations, we performed genotype-to-
384 phenotype associations at the single-gene level. For each gene and trait, we compared the three
385 classes of LOF dosages (LOF_{0/2}, LOF_{1/2}, and LOF_{2/2}) with the EDITOR 1 control. Such single-
386 gene analyses were carried out separately for all experiments conducted under WW and WD,
387 representing in total a collection of more than 1000 plants that include data on selfed, inter- and
388 intra-script crossed lines. Our goal here was to detect major gene effects.

389 Following this approach, we could detect a subset of genes for each gene family which
390 could be, at least partially, significantly responsible for the observed phenotypes (Figure 5). In
391 SCRIPT 1, phenotypes regarding increases in FLL3 and decreases in FLW3 were associated with
392 edits on DELLA orthologs *D8* and *ZmSLR2* as well as on *ZmGa2ox5* (Figure 5A). For SCRIPT 2,
393 edits in *ZmCKX4B*, *ZmCKX6* and *ZmCKX8* were related to changes in FW, FLW3 and DW
394 (Figure 5B). In the case of SCRIPT 3, LOFs in *ZmKRP5-2* and *ZmPP2C-A11* were associated
395 with increases in FW and DW, while LOF in *ZmKRP1-1*, *ZmHB124B* and *ZmHB124* correlated
396 with increases in biomass moisture (Figure 5C). Finally, for SCRIPT 4, the main genes involved
397 in the increases observed in FLW3 were *ZmTCP8*, *ZmTCP9*, *ZmTCP10*, *ZmTCP22* and
398 *ZmTCP42* (Figure 5D). Particularly, LOFs in *ZmTCP22*, *ZmTCP42* and *ZmTCP9* were associated
399 with concomitant increases in FW and moisture content, and therefore decreases in DW.
400 *ZmGRF10* and *ZmGRF4* were associated to increases in FLL3.

401 To further validate the rationale used for the associations, we analyzed in detail
402 population P012 of SCRIPT 1 (Figure 6). In this population, *D8*, one of the selected genes
403 associated to increases in FLL3 (Figure 5A), showed two haplotype_{KO}, each with an out-frame
404 indel (-1 bp and +1 bp) and an haplotype_{REF} with an in-frame indel (-3 bp) (Figure 6A). In the
405 progeny, the haplotypes segregated resulting in different LOF dosage combinations. Within that
406 population, plants containing only a LOF_{1/2} in *D8* presented similar phenotypes of FLL3 and
407 FLW3 compared with EDITOR 1, whereas plants with a LOF_{2/2} in *D8* displayed longer and
408 narrower leaves (Figure 6B-C).

409

410 Discussion

411 Complex agronomical traits such as yield or resistance to a particular (a)biotic stress are
412 governed by a large network of genes that together determine a specific phenotype.
413 Understanding the complexity of such networks is the central aspiration of systems biology.

414 Here, we developed an experimental approach, named BREEDIT, to study gene networks
415 affecting complex quantitative traits by combining multiplex CRISPR-mediated gene editing of
416 whole gene families with specific crossing schemes. In BREEDIT, a Cas9-expressing line
417 (EDITOR) is supertransformed with vectors containing 12 gRNAs (SCRIPTs) targeting a set of
418 GRGs. Gene edits are further stacked in plants using crossing schemes.

419 We evaluated the BREEDIT strategy by targeting putative players in major plant gene
420 families or pathways involved in growth regulation. The success rate of the multiplex gene
421 editing approach in maize was very high, with more than 97% of the genes showing at least
422 partial or complete LOF at T1. In just two generations, BREEDIT created multiple gene KOs
423 leading to a diverse collection of genetic profiles, from low-order mutants with one, two or three
424 gene KOs to higher-order mutants stacking mutations on up to 11 genes out of the 12 within a
425 single SCRIPT. Additional levers could be used to further increase the number of gene KOs
426 stacked in one plant, namely inter-script crosses and the ongoing Cas9 activity. We indeed
427 showed that higher-order mutants could be obtained by crossing plants already containing high
428 numbers of gene KOs at the single-SCRIPT level. Finally, the combined presence of the Cas9
429 and the SCRIPT throughout the generations enabled the CRISPR/Cas9 machinery to
430 continuously generate mutations in not yet edited loci. This ongoing Cas9 activity can therefore
431 contribute to reach saturation in gene edits after a couple of generations and increase the number
432 of gene KOs stacked in one plant. Interestingly, we noticed that while in the T0 plants often both
433 copies of the target genes carried the same or a different mutation (bi-allelic), genes newly edited
434 at T1 all showed heterozygous mutations, suggesting that only one chromosome of the two is
435 edited. We hypothesized that chromatin condensation may influence DNA accessibility for the
436 CRISPR/Cas9 machinery, possibly by imprinting (Borg and Berger, 2015). Further research is
437 needed to elaborate on the mechanisms.

438 We obtained more than 1000 plants with often different unique LOF profiles to score for
439 phenotypes. The high sensitivity of HiPlex amplicon sequencing enabled to capture complete sets
440 of haplotypes with CRISPR/Cas9 mutations in large arrays of samples and loci. We used the
441 haplotype sequence to focus on haplotypes supposed to have major effect (haplotype_{KO}) on the
442 translated protein function or activity. The experimental set-up based on multiple observations of
443 significant single-gene KO associations with phenotypes across different populations and
444 experiments enabled us to identify significant phenotypic responses in growth traits for all

445 SCRIPTs. In the case of SCRIPT 1, we observed previously known effects of elevated gibberellic
446 acid (GA) levels, such as plants with long and narrow leaves (Nelissen et al., 2012; Voorend et
447 al., 2016) as well as male sterility, a trait that was previously associated with the effect of GA on
448 tassel development (Colombo and Favret, 1996). SCRIPT 4 plants displayed an increased FLW3
449 (alongside with milder increases in FLL3), which impacted the FW in some populations. Lastly,
450 for SCRIPT 2 and SCRIPT 3, the most pronounced phenotypes observed were increased FLL3
451 and FW, particularly under WD conditions.

452 If we consider these single-SCRIPT lines as building blocks, the possibility to stack
453 several different combinations of SCRIPTs by crossing, opens the way to create higher-order
454 mutant lines that may display even stronger or additive phenotypes. The inter-script lines we
455 generated displayed higher-order mutations more than (12) and inherited traits observed in
456 parental single-SCRIPT lines. Though some of the expressed traits (e.g. increases in FW) were
457 not observed in all different inter-script populations of the same type (probably because different
458 haplotypes are segregating in different populations), some other traits (such as increases of FLW)
459 were consistently observed in all generations of lines containing SCRIPT 4, which further
460 validates the consistency of the results analyzed at single-SCRIPT level.

461 Another important outcome of the BREEDIT strategy is the possibility to screen large sets
462 of genes that are then ranked and prioritized to delineate a minimal set of LOF required to induce
463 a maximal phenotypic effect. Further inspection of the selected 48 GRGs showed that certain
464 subsets of genes are strongly associated to specific traits (or combination of traits). Using this
465 information, we built a possible regulatory network that integrates all the single-gene effects and
466 their impact over all the different measured traits (Figure 7). In this network, central genes (such
467 as *ZmCKX4B*, *ZmCKX48* and *ZmCKX46* and *ZmTCP9*, *ZmTCP10*, *ZmTCP22* and *ZmTCP42*) act
468 as nodes connected to several traits, inferring a possible broader role in regulation. The genes
469 located at the edge of the network may play a more defined role, connecting to just one or two
470 traits (such as *ZmGRF10*, *ZmGRF4*, *ZmCKX3* and *ZmTCP8*). Finally, other genes connect to
471 specific patterns, like *D8*, *SLRL2*, and *Ga2ox5*, of which LOF strongly increases the FLL3 while
472 also strongly decreasing the FLW, or *ZmHBI24B*, of which LOF influences the FW and moisture
473 positively. Therefore, using single-gene KO associations, we could identify subsets of genes per
474 family, of which LOF, alone or in combination, may be responsible for the observed phenotypes.
475 Furthermore, some of these genes were already shown to play roles in modifying agronomical

476 traits in other studies. A gain-of-function mutation in *D8* (SCRIPT 1), encoding a DELLA maize
477 protein ortholog, is causative of dwarf phenotypes (Winkler and Freeling, 1994; Lawit et al.,
478 2010). *ZmCKX-4B* (SCRIPT 2) plays a role in both drought (Rida et al., 2021) and heat shock
479 stress (Wang et al., 2020). Downregulation of *ZmHB124B* and *ZmHB124C* induces the formation
480 of additional protoxylem files in the vasculature (Bloch et al., 2019), which could prevent
481 vascular embolism and water retention under water-limiting conditions (Hwang et al., 2016).
482 *ZmGRF10* (SCRIPT 4) overexpression in maize leads to a decrease in leaf length and height (Wu
483 et al., 2014; Nelissen et al., 2015). Although these genes were highlighted in our single-gene KO
484 associations, we cannot exclude that other genes from the original pool may play minor roles,
485 either individually or in combinations, but end up masked by the effect of major gene KOs.
486 Nonetheless, this subset selection provides a valuable material pool for further research to tackle
487 specific traits (e.g. leaf width, enhanced growth under WD).

488 While applying the BREEDIT strategy to our case study in maize, we identified a couple
489 of limits to the approach. First, the inability to fully uncouple complex gene interactions. In plant
490 models where transformation and regeneration are efficient, the possibility for massive gene
491 editing grows faster than the capacity to phenotypically analyze the resulting collections of
492 mutants. For complex quantitative traits, large populations of lower-order mutants need to be
493 screened accurately to decipher the complex mechanisms underlying plant development (Liu et
494 al., 2020). To illustrate this, we have developed the following multiplex edited scenario
495 (Supplemental Figure S13). If one would be interested in exhaustively capturing both additive
496 and synergistic gene effects, all the gene KO combinations have to be generated and analyzed.
497 Considering n genes to be targeted, the number of different genetic combinations that have to be
498 produced amounts to 2^n in the case of two-state genes (homozygous wild type or homozygous
499 mutant) (Supplemental Figure S13A) and 3^n if the heterozygous stage has to be considered as
500 well. Given that at least ten replicates per genetic profile (combination) are required to
501 statistically demonstrate a 10% significant difference in FLL3 with enough statistical power
502 (Supplemental Figure S13B), the final amount of plants to be processed increases dramatically as
503 the number of genes in the study grows. Large scale phenotyping/genotyping in field conditions
504 would allow to increase the statistical power to detect combinatorial genes effects that govern
505 agronomic traits, including seed yield.

506 By applying the BREEDIT strategy on a broad gene set, one could generate a reduced
507 sub-selection of genes of interest underlying a trait and then apply complementary approaches to
508 rule out their contribution to a specific trait of interest in just two generations. One of such
509 approaches is the use of haploid induction (Chaikam et al., 2019; Jacquier et al., 2020), a
510 promising technique to create homozygous mutations, thus removing the need to consider
511 heterozygous material. This could be particularly interesting as a follow up of BREEDIT,
512 because the new gene edits that we observed at T1 were all heterozygous. Another approach is to
513 preselect plants to be phenotyped on the basis of their genetic constitution by predicting gene
514 effects with statistical models in the same fashion as for genomic selection. Such predictions can
515 be combined with the use of non-destructive seed chipping (Mills et al., 2020) to pick specific
516 gene combinations before sowing and therefore reduce the number of plants to be tested. Once
517 the gene space is lowered, the BREEDIT pipeline can be followed again to design validation
518 constructs by engineering a vector containing gRNAs targeting only the genes retained in the
519 selected subset.

520 In this study, we present the BREEDIT strategy to rapidly generate a large collection of
521 mutants in specific gene families, pathways or networks. We foresee a large potential for
522 BREEDIT combined with existing and more recent breeding approaches, such as marker-assisted
523 breeding, haploid induction, and genomic selection. Effectively implementing the concept of
524 breeding by editing using the BREEDIT pipeline still requires to overcome some practical
525 obstacles, such as the ability to transform and regenerate the plant material, obtain the desired
526 gene KOs and segregate out the original transgene construct. When these conditions are met,
527 applying the BREEDIT pipeline enables to generate many lines with specific combinations of
528 gene KOs able to modify particular traits of interest. These engineered lines could be directly
529 introduced in a hybrid breeding pipeline by crosses to elite material. The impact of favorable
530 allele combinations on complex traits could furthermore be evaluated in different genetic
531 backgrounds and across several generations to assess their heritability. In that perspective,
532 BREEDIT could significantly speed up pre-breeding activities in which pools of diverse
533 materials (wild species, landraces, commercial varieties) are usually screened for promising
534 mutations and phenotypes (Teixeira and Guimarães, 2021) that then have to be transferred into an
535 intermediate set of materials that breeders can use to create new varieties. Introgression of alleles
536 from a divergent pool of materials is often cumbersome because of cross incompatibility, low

537 seed yield quantity and quality, or persistence of a deleterious linkage drag. Provided that elite
538 materials can be transformed and regenerated, the reverse-genetics approach developed in the
539 BREEDIT pipeline can circumvent the long and tedious step of introgression and save time in the
540 development of new commercial varieties. An additional benefit of BREEDIT could be the
541 generation of large collections of plants mutated in coding or non-coding genome areas using
542 other novel CRISPR technologies such as base editing and promoter bashing to further extend the
543 repertoire of allele variability and phenotypic responses (Vats et al., 2019; Anzalone et al., 2020;
544 Gaillochet et al., 2021).

545

546 **Materials and methods**

547 **Plant material and DNA extraction**

548 The original line used for all transformation procedures was the maize inbred line B104. DNA
549 was extracted following an adapted protocol from Berendzen et al. (2005) coupled with a
550 magnetic beads purification. A piece of 1-2 cm of leaf 1 was ground in 8-strip 2-ml capacity
551 tubes (National Scientific Supply Co). After grinding and centrifugation, the supernatant was
552 mixed with magnetic beads (CleanNA), washed in 80% ethanol and dried for further processing.

553

554 **Selection of GRGs and curation of gene models**

555 We selected 48 GRGs based on the literature, in house knowledge and orthology searches (see
556 results) in version 4 of the reference maize B73 genome sequence (Jiao et al., 2017). The
557 integrative orthology viewer in PLAZA v4.5
558 (https://bioinformatics.psb.ugent.be/plaza/versions/plaza_v4_5_monocots/) was used for
559 identification of most orthologous genes, both for finding gene families from other species or for
560 identification of the corresponding maize B104 gene IDs. When required, B104 gene models
561 were manually curated using ORCAE, an online genome annotation resource
562 (<https://bioinformatics.psb.ugent.be/orcae/>). Comparison of sequences in maize lines B104 and
563 B73 was done by pairwise alignment using Geneious Prime 2020.1.2
564 (<https://www.geneious.com/prime/>). Design of the amplicons and gRNAs was performed in
565 Geneious Prime. The maize B73 genome version 4 was used to identify gRNA on-target and off-
566 target sites. gRNAs were selected with specificity score $\geq 80-85\%$, no stretch of Ts (>4), without

567 internal *Bsa*I or *Bbs*I restriction sites, which would interfere gRNA expression and/or vector
568 construction, respectively.

569

570 **Monitoring CRISPR/Cas9 edits with HiPlex amplicon sequencing**

571 Geneious Prime was used to design primers to amplify the genomic regions surrounding the
572 gRNA cutting sites. A manual selection of two amplicons per gene was done with a size range
573 between 120-150 bp. Each amplicon contained at least two gRNAs separated from either primer
574 by at least 15 bp. The amplicons were selected to target the middle of the coding sequence and to
575 not overlap. The specificity of primers was checked in the maize B73 genome version 4 and only
576 specific primers were retained (Supplemental Table S2). All primers were pooled in a HiPlex
577 amplicon sequencing assay to sequence each locus in each plant simultaneously. HiPlex library
578 preparation was performed by Floodlight Genomics facility (Knoxville, TN, USA) using the
579 MonsterPlex technology. Pilot runs of HiPlex amplicon sequencing were conducted to select the
580 best amplicon per gene (out of the two). The selection was based on amplification efficiency in
581 the HiPlex assay measured as read counts and unambiguous read-reference mapping. Per gene,
582 the overlapping gRNA was selected for cloning into the expression vector. We used SMAP
583 haplotype-window (Schaumont et al., 2022) to trim sequencing reads, identify haplotypes at each
584 locus, and calculate the respective haplotype frequency per locus per sample. SMAP haplotype-
585 window extracts haplotypes from the HiPlex sequencing reads as the entire DNA sequence
586 between the HiPlex primers per locus. Any unique DNA sequence is considered as a haplotype.
587 The total haplotype count is recorded per locus per sample and the relative haplotype frequency
588 per locus per sample is calculated. A haplotype detection threshold of at least 1% relative read
589 depth per locus per sample was set to remove possible spurious haplotypes derived from
590 amplification and/or sequencing artifacts. The nucleotide length difference between the haplotype
591 sequence and the B104 reference sequence (LDR) was used to classify the mutations into three
592 classes: SNPs (LDR = 0 but sequences are different), insertions (LDR > 0, the mutated haplotype
593 is longer than the reference haplotype), and deletions (LDR < 0, the mutated haplotype is shorter
594 than the reference haplotype). We defined haplotypes whose indel length is not a multiple of
595 three nucleotides as haplotype_{KO} because they generate a frame shift in the open reading frame
596 that likely leads to the translation of a wrong amino acid sequence downstream of the mutation,
597 and/or create a premature stop codon, both of which could disrupt the protein function or activity.

598 Haplotypes with SNPs outside the cutting site and in-frame indels are referred as to Haplotype_{REF}
599 to denote possible minor impact of their mutations on the resulting protein, which may still
600 behave as the reference protein.

601 Maize is a diploid organism in which each gene has two alleles per nucleus, each derived
602 from one of the two parents. In plant material that stably express CRISPR/Cas9 and gRNAs,
603 continuously driving gene editing, one may expect to observe mosaic tissues, i.e. patches of
604 tissues within an organ that contain different genome sequences due to non-uniform gene editing.
605 Mosaic tissues may occur both in primary transformants and subsequent generations because of
606 the initial and ongoing Cas9 activity, respectively. A single leaf sample used for DNA
607 preparation may therefore contain cells with different gene edits resulting in scoring one
608 individual with more than two alleles. The allele dosage is also affected by mosaicism. Multi-
609 allelism resulting from mosaic tissues blurs the expected 50:50 read depth ratio commonly
610 observed between the two alleles of a diploid organism. In addition, bi-allelism can be observed
611 in non-mosaic tissues, with a plant harboring two indels of a same or different nature (in-frame or
612 out-frame) following a 50:50 read depth ratio. Genotype-to-phenotype statistical associations
613 require discrete genotypic classes (absence/presence, or homozygous wild-type, heterozygous,
614 homozygous mutant). We therefore summed the relative fraction of haplotype_{KO} per locus per
615 sample to quantify how much the locus is affected by mutations leading to a LOF. The resulting
616 aggregation (Σ haplotype_{KO}) is discretized in three genotypic classes representing three dosages of
617 haplotype_{KO}: LOF_{0/2} (<15% of the read depth per locus per sample contain haplotype_{KO}), LOF_{1/2}
618 (between 40% and 60% of the read depth per locus per sample contain haplotype_{KO}), and LOF_{2/2}
619 (>85% of the read depth per locus per sample contain haplotype_{KO}). Because distinguishing
620 between these three groups is critical to analyze dosage effects associated with a particular trait,
621 any value outside of these three ranges was scored as missing genotype call during the genotype-
622 to-phenotype association analyses.

623

624 **Construction and cloning of SCRIPT vectors**

625 The gRNA entry vectors were constructed by PCR amplification with Q5 High-Fidelity DNA
626 polymerase (New England Biolabs) of the entire pGG-[B-F]-OsU3-BbsI-ccdB-BbsI-[C-G]
627 plasmids according to the manufacturer's guidelines. The primers contained an extension to insert
628 unique linkers (Torella et al., 2014) between the scaffold and OsU3 promoter (Supplemental

629 Table S3 and Supplemental Table S4). Two of the five linkers were modified to contain *NotI*
630 restriction sites to facilitate validation of the final expression vectors by restriction digest
631 (Supplemental Figure S1). Gibson assembly was performed with NEBuilder Hifi DNA Assembly
632 Mix (New England Biolabs) to circularize the PCR products into entry vectors using the
633 manufacturer's guidelines. The new entry vectors were confirmed by Sanger sequencing
634 (Mix2Seq service, Eurofins Scientific).

635 The gRNA construction and Golden Gate assembly into binary vectors was done as
636 previously described (Decaestecker et al., 2019). Briefly, paired gRNA entry vectors were
637 created by PCR amplification (Red Taq DNA Polymerase Master Mix, VWR Life Science or
638 iProof High-Fidelity DNA Polymerase, Bio-Rad Laboratories) on the template plasmid pEN-
639 2xTaU3 with primers containing the 20-nt spacer sequences and *BbsI* restriction sites. Column-
640 purified PCR products were cloned into the Golden Gate entry vectors via a Golden Gate reaction
641 using *BbsI* (New England Biolabs). All paired gRNA entry vectors were verified by Sanger
642 sequencing.

643 Expression vectors (SCRIPT 1-4; Supplemental Figure S1) were constructed by a Golden
644 Gate reaction with *BsaI* (New England Biolabs) using the paired gRNA entry vectors and a
645 destination vector as previously described (Decaestecker et al., 2019). The destination vector,
646 pGGBb-AG, contains a GreenGate destination module (AG) and a bialaphos-resistance (*bar*)
647 gene driven by the 35S promoter. The expression of each individual gRNA was alternatively
648 driven by either the rice OsU3 promoter or the wheat TaU3 promoter (Xing et al., 2014). The
649 SCRIPT vectors were transformed via heat-shock into *ccdB*-sensitive DH5 α *Escherichia coli*
650 cells, grown on LB medium containing 100 μ g/mL spectinomycin and extracted with the
651 GeneJET Plasmid Miniprep Kit (Thermo Fisher Scientific). Quality control was performed by
652 restriction digest with *NotI* (Promega). SCRIPTs were transformed into *Agrobacterium*
653 *tumefaciens* EHA 105 cells by freeze/thaw method and plated on YEB medium with 100 μ g/mL
654 rifampicin and 100 μ g/mL spectinomycin. The gRNA entry and pGGBb-AG destination vectors
655 can be obtained via <https://gatewayvectors.vib.be/>.

656

657 **Generation of EDITOR maize lines**

658 The ζ Cas9 coding sequence containing a *Zea mays*-codon optimized Cas9 (Xing et al., 2014) was
659 cloned under control of the *ZmUbi1* promoter (pZmUBIL) and NOS terminator in pEN-L4-AG-

660 R1 (Houbaert et al., 2018) using GreenGate cloning (Lampropoulos et al., 2013). The
661 transcriptional unit was recombined with pEN-L1-linker-L2 and the pHbm42GW7 destination
662 vector (Karimi et al., 2013). The resulting construct pXHb-pZmUBIL-zCas9-NOS_t allows to
663 select maize transformants with hygromycin and is referred to as the EDITOR construct.

664 The EDITOR construct was introduced into the B104 maize line using *Agrobacterium*-
665 mediated transformation of immature embryos (Coussens et al., 2012) and hygromycin as a
666 selection agent. Three independent lines (EDITOR 1 to 3) with a single-locus insertion event
667 were selected and made homozygous for the T-DNA locus by self-crossing. To measure Cas9
668 protein levels, total proteins from leaf tissue of EDITOR lines were extracted, separated by
669 polyacrylamide gel electrophoresis and blotted on PVDF membrane. For quantification, the blots
670 were stained by incubation with anti-Cas9-HRP primary antibody (Abcam, 1:5000) for 4 h and
671 detected by chemiluminescence. Blots were also Ponceau-stained for protein loading control.
672 EDITOR 1 was crossed with wild-type B104 plants to yield heterozygous immature embryos for
673 a second round of transformation (supertransformation) with each SCRIPT construct separately.
674 Backcrosses render more seeds/embryos compared to self- crosses and also facilitate the removal
675 of Cas9 in the progeny by segregation. For each SCRIPT, at least ten independent T₀
676 supertransformants following BASTA selection were obtained and genotyped by HiPlex
677 amplicon sequencing.

678

679 **Experimental design and phenotyping**

680 Maize seeds were soaked in water for 24 h and then sown in 0.3-l square pots (7×7×7 cm) using
681 ‘potgrond met meststof’ (N.V. Van Israel) as substrate. Pots were then arrayed in groups of 24 in
682 48.0- x 30.5-cm trays, randomized and placed in growth chambers with controlled temperature
683 (24°C), relative humidity (55%) and a 16:8 photoperiod with controlled light intensity (170-200
684 μmol/m²/s photosynthetic active radiation provided from a mixture of 50/50 Radium halogen
685 HRI-BT 400W/D Pro Daylight and Philips master son-t pia plus 400-W bulbs).

686 For WW conditions, plants were grown under a water regime of 2.4 g of water per g of
687 dry potting mix, while for WD assays, this was reduced to 1.1 - 1.4 g of water per g of dry potting
688 mix, which is approximately -100 kPa water potential (Verbraeken et al., 2021). The final leaf
689 length was measured at V3 (FLL3, when the collar of leaf 3 is fully developed) from the crown of
690 the plant to the leaf tip and final leaf width (FLW3) was determined at the middle point of the

691 leaf blade. For biomass, aerial parts of V3 seedlings were harvested and weighed for fresh weight
692 (FW) and then dried in a 60°C oven to estimate dry weight (DW). Biomass moisture content was
693 calculated on a DW basis as $FW-DW/DW$.

694

695 **Statistics to detect genotype-to-phenotype associations**

696 Phenotypic datasets were trimmed to remove individuals that scored as under-developed
697 (misshapen or developed less than V3 at the moment of harvest, or over-grown, i.e. that
698 surpassed V3 at the moment of sampling) during the phenotyping trials. Within each population
699 and experiment, one-way ANOVAs were then conducted at the single-gene level to check for
700 differences between the control (EDITOR 1) and mutant groups (either LOF_{1/2} or LOF_{2/2}). The
701 minimal size of a mutant group to be considered in statistical analysis was six individuals having
702 both phenotypic and genotypic data. Post-hoc HSD Tukey's tests were then performed to assign
703 each mutant group to a statistical group. Finally, we recorded the number of times a KO (either
704 LOF_{1/2} or LOF_{2/2}) of a specific gene was found to be significantly associated with a given trait
705 while leading on average to a >10% increase or decrease compared to the control line (EDITOR
706 1). We compared that count with the number of times sufficient data was available to statistically
707 conclude on a gene KO effect and defined the resulting ratio as the strength of the association.

708

709 **Accession numbers**

710 The entire set of Illumina paired-end read sequences have been deposited at the Sequence Read
711 Archive (DDBJ/ENA/GenBank) under the BioProject accession PRJNA815957.

712

713 **Competing interests**

714 The authors declare that they have no conflicts of interest.

715

716 **Supplemental data**

717 **Supplemental Figure S1.** Map of a SCRIPT construct containing 12 gRNAs.

718 **Supplemental Figure S2.** Location of the 48 growth-related genes over the 10 chromosomes
719 of maize.

720 **Supplemental Figure S3.** Cas9 protein expression levels in three different EDITOR lines.

721 **Supplemental Figure S4.** Comparative summaries of the mutations observed in plants
722 harboring SCRIPT 1 in an EDITOR 1 vs. EDITOR 3 background.

723 **Supplemental Figure S5.** Haplotype overview in T0 material from the four SCRIPTs.

724 **Supplemental Figure S6.** Distribution of the aggregated frequency of haplotypes with out-
725 frame indels (Σ Haplotype KO) in the ingroup samples.

726 **Supplemental Figure S7.** Appearance of new indels in inter-script crosses.

727 **Supplemental Figure S8.** Phenotypes of mutated populations for the four SCRIPTs.

728 **Supplemental Figure S9.** Sterility phenotypes observed in tassels of SCRIPT 1 T0 plants.

729 **Supplemental Figure S10.** Characteristic phenotypes observed in T1 plants of SCRIPT 2
730 under water-deficient conditions.

731 **Supplemental Figure S11.** Characteristic phenotypes observed in T1 plants of SCRIPT 3
732 under water-deficient conditions.

733 **Supplemental Figure S12.** Phenotypes of mutated inter-script populations.

734 **Supplemental Figure S13.** Considerations on numbers for multiplex gene editing
735 experiments.

736 **Supplemental Table S1.** Detailed information of populations used in the phenotyping assays.

737 **Supplemental Table S2.** List of gRNAs and associated primer pairs for edit detection using
738 HiPlex amplicon sequencing.

739 **Supplemental Table S3.** Plasmid overview.

740 **Supplemental Table S4.** Primers used for plasmid building and sequencing.

741

742 **Acknowledgments**

743 The authors would like to thank Lieven Sterck for helping in gene model curation, Mansour
744 Karimi for helping with the cloning of EDITOR constructs, Pan Gong, Reinout Laureyns, and Ji
745 Li for additional help with the selection of the genes.

746

747 **Funding**

748 This work was supported by the European Research Council (ERC) under the European Union's
749 Horizon 2020 Research and Innovation Programme (H2020/2019-2025) under grant agreement
750 No 833866-BREEDIT.

751

752 **References**

753

- 754 **Anzalone AV, Koblan LW, and Liu DR.** (2020). Genome editing with CRISPR-Cas nucleases, base
755 editors, transposases and prime editors. *Nat. Biotechnol.* **38**: 824-844
- 756 **Ashikari M, Sakakibara H, Lin S, Yamamoto T, Takashi T, Nishimura A, Angeles ER, Qian Q,**
757 **Kitano H, and Matsuoka M.** (2005). Cytokinin oxidase regulates rice grain production. *Science*
758 **309**: 741-745
- 759 **Bai M, Yuan J, Kuang H, Gong P, Li S, Zhang Z, Liu B, Sun J, Yang M, Yang L, et al.** (2020).
760 Generation of a multiplex mutagenesis population via pooled CRISPR-Cas9 in soya bean. *Plant*
761 *Biotechnol. J.* **18**: 721-731
- 762 **Bartrina I, Otto E, Strnad M, Werner T, and Schmülling T.** (2011). Cytokinin regulates the activity of
763 reproductive meristems, flower organ size, ovule formation, and thus seed yield in *Arabidopsis*
764 *thaliana*. *Plant Cell* **23**: 69-80
- 765 **Baute J, Herman D, Coppens F, De Block J, Slabbinck B, Dell'Acqua M, Pè ME, Maere S, Nelissen**
766 **H, and Inzé D.** (2015). Correlation analysis of the transcriptome of growing leaves with mature
767 leaf parameters in a maize RIL population. *Genome Biol.* **16**: 168
- 768 **Baute J, Herman D, Coppens F, De Block J, Slabbinck B, Dell'Acqua M, Pè ME, Maere S, Nelissen**
769 **H, and Inzé D.** (2016). Combined large-scale phenotyping and transcriptomics in maize reveals a
770 robust growth regulatory network. *Plant Physiol.* **170**: 1848-1867
- 771 **Berendzen K, Searle I, Ravenscroft D, Koncz C, Batschauer A, Coupland G, Somssich IE, and**
772 **Ülker B.** (2005). A rapid and versatile combined DNA/RNA extraction protocol and its
773 application to the analysis of a novel DNA marker set polymorphic between *Arabidopsis thaliana*
774 ecotypes Col-0 and Landsberg *erecta*. *Plant Methods* **1**: 4
- 775 **Bhat JA, Yu D, Bohra A, Ganie SA, and Varshney RK.** (2021). Features and applications of haplotypes
776 in crop breeding. *Commun. Biol.* **4**: 1266
- 777 **Bloch D, Puli MR, Mosquna A, and Yalovsky S.** (2019). Abiotic stress modulates root patterning via
778 ABA-regulated microRNA expression in the endodermis initials. *Development* **146**: dev177097

- 779 **Borg M, and Berger F.** (2015). Chromatin remodelling during male gametophyte development. *Plant J.*
780 **83:** 177-188
- 781 **Brás TA, Seixas J, Carvalhais N, and Jägermeyr J.** (2021). Severity of drought and heatwave crop
782 losses tripled over the last five decades in Europe. *Environ. Res. Lett.* **16:** 065012
- 783 **Cao L, Wang S, Venglat P, Zhao L, Cheng Y, Ye S, Qin Y, Datla R, Zhou Y, and Wang H.** (2018).
784 *Arabidopsis* ICK/KRP cyclin-dependent kinase inhibitors function to ensure the formation of one
785 megaspore mother cell and one functional megaspore per ovule. *PLoS Genet.* **14:** e1007230
- 786 **Chaikam V, Molenaar W, Melchinger AE, and Boddupalli PM.** (2019). Doubled haploid technology
787 for line development in maize: technical advances and prospects. *Theor. Appl. Genet.* **132:** 3227-
788 3243
- 789 **Cheng Y, Cao L, Wang S, Li Y, Shi X, Liu H, Li L, Zhang Z, Fowke LC, Wang H, et al.** (2013).
790 Downregulation of multiple CDK inhibitor *ICK/KRP* genes upregulates the E2F pathway and
791 increases cell proliferation, and organ and seed sizes in *Arabidopsis*. *Plant J.* **75:** 642-655
- 792 **Colombo N, and Favret EA.** (1996). The effect of gibberellic acid on male fertility in bread wheat.
793 *Euphytica* **91:** 297-303
- 794 **Coussens G, Aesaert S, Verelst W, Demeulenaere M, De Buck S, Njuguna E, Inzé D, and Van**
795 **Lijsebettens M.** (2012). *Brachypodium distachyon* promoters as efficient building blocks for
796 transgenic research in maize. *J. Exp. Bot.* **63:** 4263-4273
- 797 **Czesnick H, and Lenhard M.** (2015). Size control in plants—lessons from leaves and flowers. *Cold*
798 *Spring Harb. Perspect. Biol.* **7:** a019190
- 799 **Decaestecker W, Andrade Buono R, Pfeiffer ML, Vangheluwe N, Jourquin J, Karimi M, Van**
800 **Isterdael G, Beeckman T, Nowack MK, and Jacobs TB.** (2019). CRISPR-TSKO: a technique
801 for efficient mutagenesis in specific cell types, tissues, or organs in *Arabidopsis*. *Plant Cell* **31:**
802 2868-2887
- 803 **Doll NM, Gilles LM, Gerentes M-F, Richard C, Just J, Fierlej Y, Borrelli VMG, Gendrot G, Ingram**
804 **GC, Rogowsky PM, et al.** (2019). Single and multiple gene knockouts by CRISPR–Cas9 in
805 maize. *Plant Cell Rep.* **38:** 487-501
- 806 **Elias F, Muleta D, and Woyessa D.** (2016). Effects of phosphate solubilizing fungi on growth and yield
807 of haricot bean (*Phaseolus vulgaris* L.) plants. *J. Agric. Sci.* **8:** 204-218
- 808 **Gaillochet C, Develtere W, and Jacobs TB.** (2021). CRISPR screens in plants: approaches, guidelines,
809 and future prospects. *Plant Cell* **33:** 794-813
- 810 **Gong P, Bontinck M, Demuyneck K, De Block J, Gevaert K, Eeckhout D, Persiau G, Aesaert S,**
811 **Coussens G, Van Lijsebettens M, et al.** (2022). SAMBA controls cell division rate during maize
812 development. *Plant Physiol.* **188:** 411-424
- 813 **Gong R, Cao H, Zhang J, Xie K, Wang D, and Yu S.** (2018). Divergent functions of the GAGA-binding
814 transcription factor family in rice. *Plant J.* **94:** 32-47
- 815 **Gonzalez N, Vanhaeren H, and Inzé D.** (2012). Leaf size control: complex coordination of cell division
816 and expansion. *Trends Plant Sci.* **17:** 332-340
- 817 **Hai NN, Chuong NN, Tu NHC, Kisiala A, Hoang XLT, and Thao NP.** (2020). Role and regulation of
818 cytokinins in plant response to drought stress. *Plants* **9:** 422
- 819 **He Z, Wu J, Sun X, and Dai M.** (2019). The maize clade A PP2C phosphatases play critical roles in
820 multiple abiotic stress responses. *Int. J. Mol. Sci.* **20:** 3573
- 821 **Houbaert A, Zhang C, Tiwari M, Wang K, de Marcos Serrano A, Savatin DV, Urs MJ, Zhiponova**
822 **MK, Gudesblat GE, Vanhoutte I, et al.** (2018). POLAR-guided signalling complex assembly
823 and localization drive asymmetric cell division. *Nature* **563:** 574-578
- 824 **Huang Y, Wang X, Ge S, and Rao G-Y.** (2015). Divergence and adaptive evolution of the gibberellin
825 oxidase genes in plants. *BMC Evol. Biol.* **15:** 207
- 826 **Hwang BG, Ryu J, and Lee SJ.** (2016). Vulnerability of protoxylem and metaxylem vessels to
827 embolisms and radial refilling in a vascular bundle of maize leaves. *Front. Plant Sci.* **7:** 941
- 828 **Ikeda A, Ueguchi-Tanaka M, Sonoda Y, Kitano H, Koshioka M, Futsuhara Y, Matsuoka M, and**
829 **Yamaguchi J.** (2001). *slender rice*, a constitutive gibberellin response mutant, is caused by a null

- 830 mutation of the *SLRI* gene, an ortholog of the height-regulating gene *GAI/RGA/RHT/D8*. *Plant*
831 *Cell* **13**: 999-1010
- 832 **Impens L, Jacobs TB, Nelissen H, Inz2 D, and Pauwels L.** (2022). Mini-Review: Transgenerational
833 CRISPR/Cas9 gene editing in plants. *Frontiers in Genome Editing* **4**: 825042
- 834 **Itoh H, Shimada A, Ueguchi-Tanaka M, Kamiya N, Hasegawa Y, Ashikari M, and Matsuoka M.**
835 (2005). Overexpression of a GRAS protein lacking the DELLA domain confers altered gibberellin
836 responses in rice. *Plant J.* **44**: 669-679
- 837 **Jacobs TB, Zhang N, Patel D, and Martin GB.** (2017). Generation of a collection of mutant tomato
838 lines using pooled CRISPR libraries. *Plant Physiol.* **174**: 2023-2037
- 839 **Jacquier NMA, Gilles LM, Pyott DE, Martinant J-P, Rogowsky PM, and Widiez T.** (2020). Puzzling
840 out plant reproduction by haploid induction for innovations in plant breeding. *Nat. Plants* **6**: 610-
841 619
- 842 **Jiao Y, Peluso P, Shi J, Liang T, Stitzer MC, Wang B, Campbell MS, Stein JC, Wei X, Chin C-S, et**
843 **al.** (2017). Improved maize reference genome with single-molecule technologies. *Nature* **546**:
844 524-527
- 845 **Karimi M, Inzé D, Van Lijsebettens M, and Hilson P.** (2013). Gateway vectors for transformation of
846 cereals. *Trends Plant Sci.* **18**: 1-4
- 847 **Knott GJ, and Doudna JA.** (2018). CRISPR-Cas guides the future of genetic engineering. *Science* **361**:
848 866-869
- 849 **Koyama T, Sato F, and Ohme-Takagi M.** (2017). Roles of miR319 and TCP transcription factors in leaf
850 development. *Plant Physiol.* **175**: 874-885
- 851 **Lampropoulos A, Sutikovic Z, Wenzl C, Maegle I, Lohmann JU, and Forner J.** (2013). GreenGate -
852 A novel, versatile, and efficient cloning system for plant transgenesis. *PLoS ONE* **8**: e83043
- 853 **Lan J, and Qin G.** (2020). The regulation of CIN-like TCP transcription factors. *Int. J. Mol. Sci.* **21**:
854 4498
- 855 **Lawit SJ, Wych HM, Xu D, Kundu S, and Tomes DT.** (2010). Maize DELLA Proteins dwarf plant8
856 and dwarf plant9 as Modulators of Plant Development. *Plant and Cell Physiology* **51**: 1854-1868
- 857 **Li C, Hao M, Wang W, Wang H, Chen F, Chu W, Zhang B, Mei D, Cheng H, and Hu Q.** (2018). An
858 efficient CRISPR/Cas9 platform for rapidly generating simultaneous mutagenesis of multiple
859 gene homoeologs in allotetraploid oilseed rape. *Front. Plant Sci.* **9**: 442
- 860 **Li J, Wang Z, He G, Ma L, and Deng XW.** (2020). CRISPR/Cas9-mediated disruption of *TaNPI* genes
861 results in complete male sterility in bread wheat. *J. Genet. Genomics* **47**: 263-272
- 862 **Li N, and Li Y.** (2016). Signaling pathways of seed size control in plants. *Curr. Opin. Plant Biol.* **33**: 23-
863 32
- 864 **Li W, Herrera-Estrella L, and Tran L-SP.** (2016). The yin–yang of cytokinin homeostasis and drought
865 acclimation/adaptation. *Trends Plant Sci.* **21**: 548-550
- 866 **Li Y, Shan X, Jiang Z, Zhao L, and Jin F.** (2021). Genome-wide identification and expression analysis
867 of the *GA2ox* gene family in maize (*Zea mays* L.) under various abiotic stress conditions. *Plant*
868 *Physiol. Biochem.* **166**: 621-633
- 869 **Liebsch D, and Palatnik JF.** (2020). MicroRNA miR396, GRF transcription factors and GIF co-
870 regulators: a conserved plant growth regulatory module with potential for breeding and
871 biotechnology. *Curr. Opin. Plant Biol.* **53**: 31-42
- 872 **Liu H-J, Jian L, Xu J, Zhang Q, Zhang M, Jin M, Peng Y, Yan J, Han B, Liu J, et al.** (2020). High-
873 throughput CRISPR/Cas9 mutagenesis streamlines trait gene identification in maize. *Plant Cell*
874 **32**: 1397-1413
- 875 **Liu L, Gallagher J, Arevalo ED, Chen R, Skopelitis T, Wu Q, Bartlett M, and Jackson D.** (2021).
876 Enhancing grain-yield-related traits by CRISPR–Cas9 promoter editing of maize *CLE* genes. *Nat.*
877 *Plants* **7**: 287-294
- 878 **Long SP, Marshall-Colon A, and Zhu X-G.** (2015). Meeting the global food demand of the future by
879 engineering crop photosynthesis and yield potential. *Cell* **161**: 56-66

- 880 **Lu Y, Ye X, Guo R, Huang J, Wang W, Tang J, Tan L, Zhu J-k, Chu C, and Qian Y.** (2017).
881 Genome-wide targeted mutagenesis in rice using the CRISPR/Cas9 system. *Mol. Plant* **10**: 1242-
882 1245
- 883 **McConnell JR, Emery J, Eshed Y, Bao N, Bowman J, and Barton MK.** (2001). Role of *PHABULOSA*
884 and *PHAVOLUTA* in determining radial patterning in shoots. *Nature* **411**: 709-713
- 885 **Meng X, Yu H, Zhang Y, Zhuang F, Song X, Gao S, Gao C, and Li J.** (2017). Construction of a
886 genome-wide mutant library in rice using CRISPR/Cas9. *Mol. Plant* **10**: 1238-1241
- 887 **Mickelbart MV, Hasegawa PM, and Bailey-Serres J.** (2015). Genetic mechanisms of abiotic stress
888 tolerance that translate to crop yield stability. *Nat. Rev. Genet.* **16**: 237-251
- 889 **Miculan M, Nelissen H, Hassen MB, Marroni F, Inzé D, Pè ME, and Dell'Acqua M.** (2021). A
890 forward genetics approach integrating genome-wide association study and expression quantitative
891 trait locus mapping to dissect leaf development in maize (*Zea mays*). *Plant J.* **107**: 1056-1071
- 892 **Mills A, Allsman L, Leon S, and Rasmussen C.** (2020). Using seed chipping to genotype maize kernels.
893 *Bio-Protocol* **101**: e3553
- 894 **Nelissen H, Rymen B, Jikumaru Y, Demuynck K, Van Lijsebettens M, Kamiya Y, Inzé D, and**
895 **Beemster GTS.** (2012). A local maximum in gibberellin levels regulates maize leaf growth by
896 spatial control of cell division. *Curr. Biol.* **22**: 1183-1187
- 897 **Nelissen H, Eeckhout D, Demuynck K, Persiau G, Walton A, van Bel M, Vervoort M, Candaele J,**
898 **De Block J, Aesaert S, et al.** (2015). Dynamic changes in *ANGUSTIFOLIA3* complex
899 composition reveal a growth regulatory mechanism in the maize leaf. *Plant Cell* **27**: 1605-1619
- 900 **Nuccio ML, Paul M, Bate NJ, Cohn J, and Cutler SR.** (2018). Where are the drought tolerant crops?
901 An assessment of more than two decades of plant biotechnology effort in crop improvement. *Plant*
902 *Sci.* **273**: 110-119
- 903 **Paul BK, Frelat R, Birnholz C, Ebong C, Gahigi A, Groot JCJ, Herrero M, Kagabo DM,**
904 **Notenbaert A, Vanlauwe B, et al.** (2018). Agricultural intensification scenarios, household food
905 availability and greenhouse gas emissions in Rwanda: Ex-ante impacts and trade-offs. *Agric. Syst.*
906 **163**: 16-26
- 907 **Poland J, and Rutkoski J.** (2016). Advances and challenges in genomic selection for disease resistance.
908 *Annu. Rev. Phytopathol.* **54**: 79-98
- 909 **Qin F, Kodaira K-S, Maruyama K, Mizoi J, Tran L-SP, Fujita Y, Morimoto K, Shinozaki K, and**
910 **Yamaguchi-Shinozaki K.** (2011). *SPINDLY*, a negative regulator of gibberellic acid signaling, is
911 involved in the plant abiotic stress response. *Plant Physiol.* **157**: 1900-1913
- 912 **Ramadan M, Alariqi M, Ma Y, Li Y, Liu Z, Zhang R, Jin S, Min L, and Zhang X.** (2021). Efficient
913 CRISPR/Cas9 mediated pooled-sgRNAs assembly accelerates targeting multiple genes related to
914 male sterility in cotton. *Plant Methods* **17**: 16
- 915 **Rasheed A, Hao Y, Xia X, Khan A, Xu Y, Varshney RK, and He Z.** (2017). Crop breeding chips and
916 genotyping platforms: progress, challenges, and perspectives. *Mol. Plant* **10**: 1047-1064
- 917 **Rida S, Maafi O, López-Malvar A, Revilla P, Riache M, and Djemel A.** (2021). Genetics of
918 germination and seedling traits under drought stress in a MAGIC population of maize. *Plants* **10**:
919 1786
- 920 **Rodríguez-Leal D, Lemmon ZH, Man J, Bartlett ME, and Lippman ZB.** (2017). Engineering
921 quantitative trait variation for crop improvement by genome editing. *Cell* **171**: 470-480.e478
- 922 **Sarvepalli K, and Nath U.** (2018). CIN-TCP transcription factors: transiting cell proliferation in plants.
923 *IUBMB Life* **70**: 718-731
- 924 **Schaumont D, Veeckman E, Van der Jeugt F, Haegeman A, Glabeke Sv, Bawin Y, Lukasiewicz J,**
925 **Blugeon S, Barre P, de la O. Leyva-Pérez M, et al.** (2022). Stack Mapping Anchor Points
926 (SMAP): a versatile suite of tools for read-backed haplotyping. *bioRxiv* **2022.03.10.483555**
- 927 **Simmons CR, Lafitte HR, Reimann KS, Brugière N, Roesler K, Albertsen MC, Greene TW, and**
928 **Habben JE.** (2021). Successes and insights of an industry biotech program to enhance maize
929 agronomic traits. *Plant Sci.* **307**: 110899

- 930 **Snowdon RJ, Wittkop B, Chen T-W, and Stahl A.** (2021). Crop adaptation to climate change as a
931 consequence of long-term breeding. *Theor. Appl. Genet.* **134**: 1613-1623
- 932 **Sun X, Cahill J, Van Hautegeem T, Feys K, Whipple C, Novák O, Delbare S, Versteede C, Demuynck**
933 **K, De Block J, et al.** (2017). Altered expression of maize *PLASTOCHRON1* enhances biomass
934 and seed yield by extending cell division duration. *Nat. Commun.* **8**: 14752
- 935 **Teixeira FF, and Guimarães CT.** (2021). Chapter 5 - Maize genetic resources and pre-breeding. In *Wild*
936 *Germplasm for Genetic Improvement in Crop Plants*, M.T. Azhar and S.H. Wani, eds (London,
937 United Kingdom: Academic Press, Elsevier), pp. 81-99
- 938 **Torella JP, Lienert F, Boehm CR, Chen J-H, Way JC, and Silver PA.** (2014). Unique nucleotide
939 sequence-guided assembly of repetitive DNA parts for synthetic biology applications. *Nat.*
940 *Protoc.* **9**: 2075-2089
- 941 **Vanhaeren H, Nam Y-J, De Milde L, Chae E, Storme V, Weigel D, Gonzalez N, and Inzé D.** (2017).
942 Forever young: the role of ubiquitin receptor DA1 and E3 ligase Big Brother in controlling leaf
943 growth and development. *Plant Physiol.* **173**: 1269-1282
- 944 **Vanhaeren H, Gonzalez N, Coppens F, De Milde L, Van Daele T, Vermeersch M, Eloy NB, Storme**
945 **V, and Inzé D.** (2014). Combining growth-promoting genes leads to positive epistasis in
946 *Arabidopsis thaliana*. *eLife* **3**: e02252
- 947 **Vats S, Kumawat S, Kumar V, Patil GB, Joshi T, Sonah H, Sharma TR, and Deshmukh R.** (2019).
948 Genome editing in plants: exploration of technological advancements and challenges. *Cells* **8**:
949 1386
- 950 **Verbraeken L, Wuyts N, Mertens S, Cannoot B, Maleux K, Demuynck K, De Block J, Merchie J,**
951 **Dhondt S, Bonaventure G, et al.** (2021). Drought affects the rate and duration of organ growth
952 but not inter-organ growth coordination. *Plant Physiol.* **186**: 1336-1353
- 953 **Vercruyse J, Baekelandt A, Gonzalez N, and Inzé D.** (2020). Molecular networks regulating cell
954 division during Arabidopsis leaf growth. *J. Exp. Bot.* **71**: 2365-2378
- 955 **Voorend W, Nelissen H, Vanholme R, De Vliegheer A, Van Breusegem F, Boerjan W, Roldán-Ruiz I,**
956 **Muyllé H, and Inzé D.** (2016). Overexpression of *GA20-OXIDASE1* impacts plant height,
957 biomass allocation and saccharification efficiency in maize. *Plant Biotechnol. J.* **14**: 997-1007
- 958 **Voss-Fels K, and Snowdon RJ.** (2016). Understanding and utilizing crop genome diversity via high-
959 resolution genotyping. *Plant Biotechnol. J.* **14**: 1086-1094
- 960 **Wang B, Li N, Huang S, Hu J, Wang Q, Tang Y, Yang T, Asmutola P, Wang J, and Yu Q.** (2021).
961 Enhanced soluble sugar content in tomato fruit using CRISPR/Cas9-mediated *SIINVINH1* and
962 *SIVPE5* gene editing. *PeerJ* **9**: e12478
- 963 **Wang H-Q, Liu P, Zhang J-W, Zhao B, and Ren B-Z.** (2020). Endogenous hormones inhibit
964 differentiation of young ears in maize (*Zea mays* L.) under heat stress. *Front. Plant Sci.* **11**:
965 533046
- 966 **Wang H, and Qin F.** (2017). Genome-wide association study reveals natural variations contributing to
967 drought resistance in crops. *Front. Plant Sci.* **8**: 1110
- 968 **Winkler RG, and Freeling M.** (1994). Physiological genetics of the dominant gibberellin-nonresponsive
969 maize dwarfs, *Dwarf8* and *Dwarf9*. *Planta* **193**: 341-348
- 970 **Wu L, Zhang D, Xue M, Qian J, He Y, and Wang S.** (2014). Overexpression of the maize *GRF10*, an
971 endogenous truncated growth-regulating factor protein, leads to reduction in leaf size and plant
972 height. *J. Integr. Plant Biol.* **56**: 1053-1063
- 973 **Xiao Y, Tong H, Yang X, Xu S, Pan Q, Qiao F, Raihan MS, Luo Y, Liu H, Zhang X, et al.** (2016).
974 Genome-wide dissection of the maize ear genetic architecture using multiple populations. *New*
975 *Phytol.* **210**: 1095-1106
- 976 **Xing H-L, Dong L, Wang Z-P, Zhang H-Y, Han C-Y, Liu B, Wang X-C, and Chen Q-J.** (2014). A
977 CRISPR/Cas9 toolkit for multiplex genome editing in plants. *BMC Plant Biol.* **14**: 327
- 978 **Zhang X, and Cai X.** (2011). Climate change impacts on global agricultural land availability. *Environ.*
979 *Res. Lett.* **6**: 014014

980 **Zhang Y, Malzahn AA, Sretenovic S, and Qi Y.** (2019). The emerging and uncultivated potential of
981 CRISPR technology in plant science. *Nat. Plants* **5**: 778-794

982 **Table 1. List of the 48 GRGs targeted by different SCRIPTs**

SCRIPT	Position	Gene	Gene family/pathway	B73 V3 gene id	References
1	1	<i>ZmGa2ox2</i>	GA2-oxidases	GRMZM2G006964	
1	2	<i>ZmGa2ox4</i>	GA2-oxidases	GRMZM2G153359	
1	3	<i>ZmGa2ox5</i>	GA2-oxidases	GRMZM2G176963	
1	4	<i>ZmGa2ox7</i>	GA2-oxidases	GRMZM2G427618	(Huang et al., 2015; Li et al., 2021)
1	5	<i>ZmGa2ox8</i>	GA2-oxidases	GRMZM2G155686	
1	6	<i>ZmGa2ox9</i>	GA2-oxidases	GRMZM2G152354	
1	7	<i>ZmGa2ox13</i>	GA2-oxidases	GRMZM2G031432	
1	8	<i>D8</i>	DELLA/GRAS family	GRMZM2G144744	(Winkler and Freeling, 1994; Lawit et al., 2010)
1	9	<i>D9</i>	DELLA/GRAS family	GRMZM2G024973	
1	10	<i>ZmSLRL1-1</i>	DELLA/GRAS family	GRMZM5G826526	(Ikeda et al., 2001; Itoh et al., 2005)
1	11	<i>ZmSLRL2</i>	DELLA/GRAS family	GRMZM5G874545	
1	12	<i>ZmSPY</i>	GA signalling	GRMZM2G357804	(Qin et al., 2011)
2	1	<i>ZmCKX-2</i>	cytokinin oxidases	GRMZM2G050997	
2	2	<i>ZmCKX-3</i>	cytokinin oxidases	GRMZM2G167220	
2	3	<i>ZmCKX-4</i>	cytokinin oxidases	GRMZM5G817173	
2	4	<i>ZmCKX-4B</i>	cytokinin oxidases	GRMZM2G024476	
2	5	<i>ZmCKX-5</i>	cytokinin oxidases	GRMZM2G325612	
2	6	<i>ZmCKX-6</i>	cytokinin oxidases	GRMZM2G404443	(Ashikari et al., 2005; Bartrina et al., 2011)
2	7	<i>ZmCKX-7</i>	cytokinin oxidases	GRMZM2G134634	
2	8	<i>ZmCKX-8</i>	cytokinin oxidases	GRMZM2G162048	
2	9	<i>ZmCKX-9</i>	cytokinin oxidases	GRMZM2G303707	
2	10	<i>ZmCKX-10</i>	cytokinin oxidases	GRMZM2G348452	
2	11	<i>ZmCKX-11</i>	cytokinin oxidases	GRMZM2G122340	
2	12	<i>ZmCKX-12</i>	cytokinin oxidases	GRMZM2G008792	
3	1	<i>ZmKRP1;1</i>	ICK/KRP cyclin-dependent kinase	GRMZM2G101613	
3	2	<i>ZmKRP1;2</i>	ICK/KRP cyclin-dependent kinase	GRMZM2G084570	
3	3	<i>ZmKRP1;3</i>	ICK/KRP cyclin-dependent kinase	GRMZM2G343769	
3	4	<i>ZmKRP3</i>	ICK/KRP cyclin-dependent kinase	GRMZM2G154414	(Cheng et al., 2013; Cao et al., 2018)
3	5	<i>ZmKRP4;2A</i>	ICK/KRP cyclin-dependent kinase	GRMZM2G037926	
3	6	<i>ZmKRP4;2B</i>	ICK/KRP cyclin-dependent kinase	GRMZM2G116885	
3	7	<i>ZmKRP5;1</i>	ICK/KRP cyclin-dependent kinase	GRMZM2G358931	
3	8	<i>ZmKRP5;2</i>	ICK/KRP cyclin-dependent kinase	GRMZM2G157510	
3	9	<i>ZmPP2C-A9</i>	ABA signal transduction	GRMZM2G134628	(He et al., 2019)
3	10	<i>ZmPP2C-A11</i>	ABA signal transduction	GRMZM2G159811	
3	11	<i>ZmHB124B</i>	Homeobox transcription factor family	GRMZM2G023291	(McConnell et al., 2001)
3	12	<i>ZmHB124C</i>	Homeobox transcription factor family	GRMZM2G178102	
4	1	<i>ZmTCP3</i>	TCP - CIN clade	GRMZM2G115516	
4	2	<i>ZmTCP8</i>	TCP - CIN clade	GRMZM2G020805	
4	3	<i>ZmTCP9</i>	TCP - CIN clade	GRMZM2G589470	
4	4	<i>ZmTCP10</i>	TCP - CIN clade	GRMZM2G166946	(Koyama et al., 2017; Sarvepalli and Nath, 2018; Lan and Qin, 2020)
4	5	<i>ZmTCP22</i>	TCP - CIN clade	GRMZM2G120151	
4	6	<i>ZmTCP25</i>	TCP - CIN clade	GRMZM2G035944	
4	7	<i>ZmTCP42</i>	TCP - CIN clade	GRMZM2G180568	
4	8	<i>ZmGRF4</i>	Growth-regulating factor clade	GRMZM2G004619	(Nelissen et al., 2012; Voorend et al., 2016; Liebsch and Palatnik, 2020)
4	9	<i>ZmGRF10</i>	Growth-regulating factor clade	GRMZM2G096709	
4	10	<i>ZmGRF17</i>	Growth-regulating factor clade	GRMZM2G124566	
4	11	<i>ZmPHD8</i>	SET domain transcription factor	GRMZM2G409224	-
4	12	<i>ZmBPC6</i>	GAGA-binding protein	GRMZM2G118690	(Gong et al., 2018)

983

984

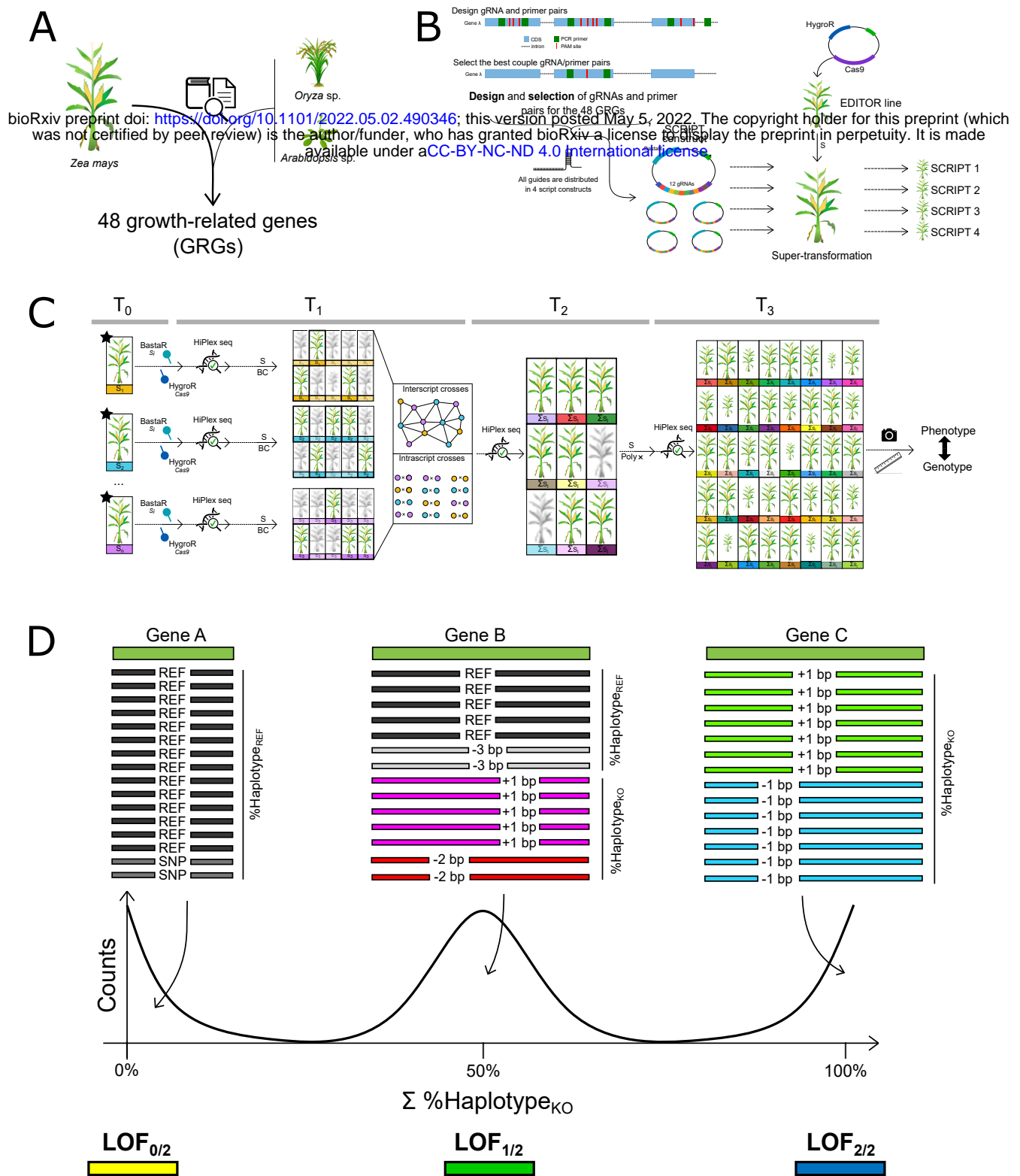


Figure 1. The multiplex gene editing strategy of BREEDIT. **A**. Selection of growth-related genes (GRGs) is based on published and in-house research performed in Arabidopsis, rice or maize **B**. After gene selection, gRNAs with NGG PAM sites are selected for each gene and PCR primer pairs are designed to re-sequence gRNA target sites and flanking regions via HiPlex amplicon sequencing. Per gene, the best set of gRNA and flanking primer pairs is selected. Twelve gRNAs are cloned in multiplex gene editing vectors named “SCRIPTS”. Next, the SCRIPT constructs are transformed in a Cas9-expressing maize line named EDITOR. **C**. Vigorous T₀ plants containing the SCRIPT (BASTA resistant) and the Cas9 EDITOR construct (hygromycin resistant) are further genotyped using HiPlex amplicon sequencing. Based on the genotypes, plants are selected either for crossing with B104 (BC: backcross), with plants with complementary mutations caused by the same SCRIPT (intra-script crosses) or with plants containing a different SCRIPT and therefore mutations in genes from a different family or pathway (inter-script crosses). These crosses aim at maximizing the mutation landscape and diversity. Finally, self-crosses (S) of lines generate a segregating progeny for high-throughput phenotyping of selected traits, which later can be associated to (combinations of) genes. **D**. From continuous read depth to discrete loss-of-function (LOF) genotypic classes. Sequencing reads are mapped to the B104 reference loci. Two read categories are derived, namely haplotype_{REF} and haplotype_{KO}. Haplotype_{REF} corresponds to the aggregated fraction of reads containing only SNPs, in-frame indels or being the reference haplotype. Haplotype_{KO} refers to the aggregated fraction of reads with out-frame indels. A tri-modal distribution is expected for haplotype_{KO}, with local maxima around 0%, 50%, 100%, each corresponding to a fraction of the genome being edited at the locus. Haplotype_{KO} is therefore discretized in three gradual classes of LOF: LOF_{0/2} (the genome is not edited with out-frame indels, i.e. 0 chromosome out of 2 in a diploid organism), LOF_{1/2} (half of the genome is edited with out-frame indels, i.e. 1 chromosome out of 2 in a diploid organism), LOF_{2/2} (all the genome is edited with out-frame indels, i.e. 2 chromosomes out of 2 in a diploid organism).

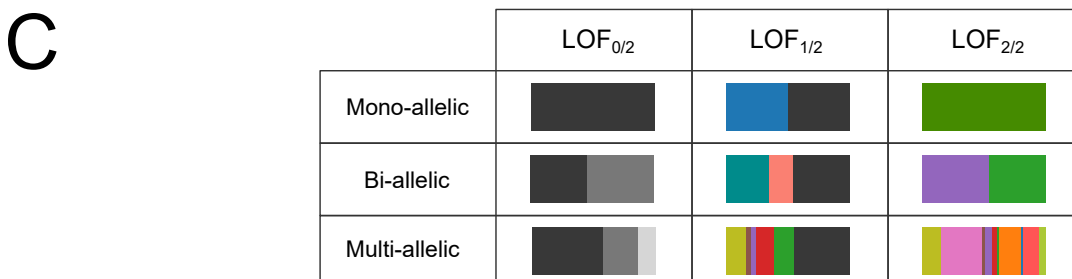
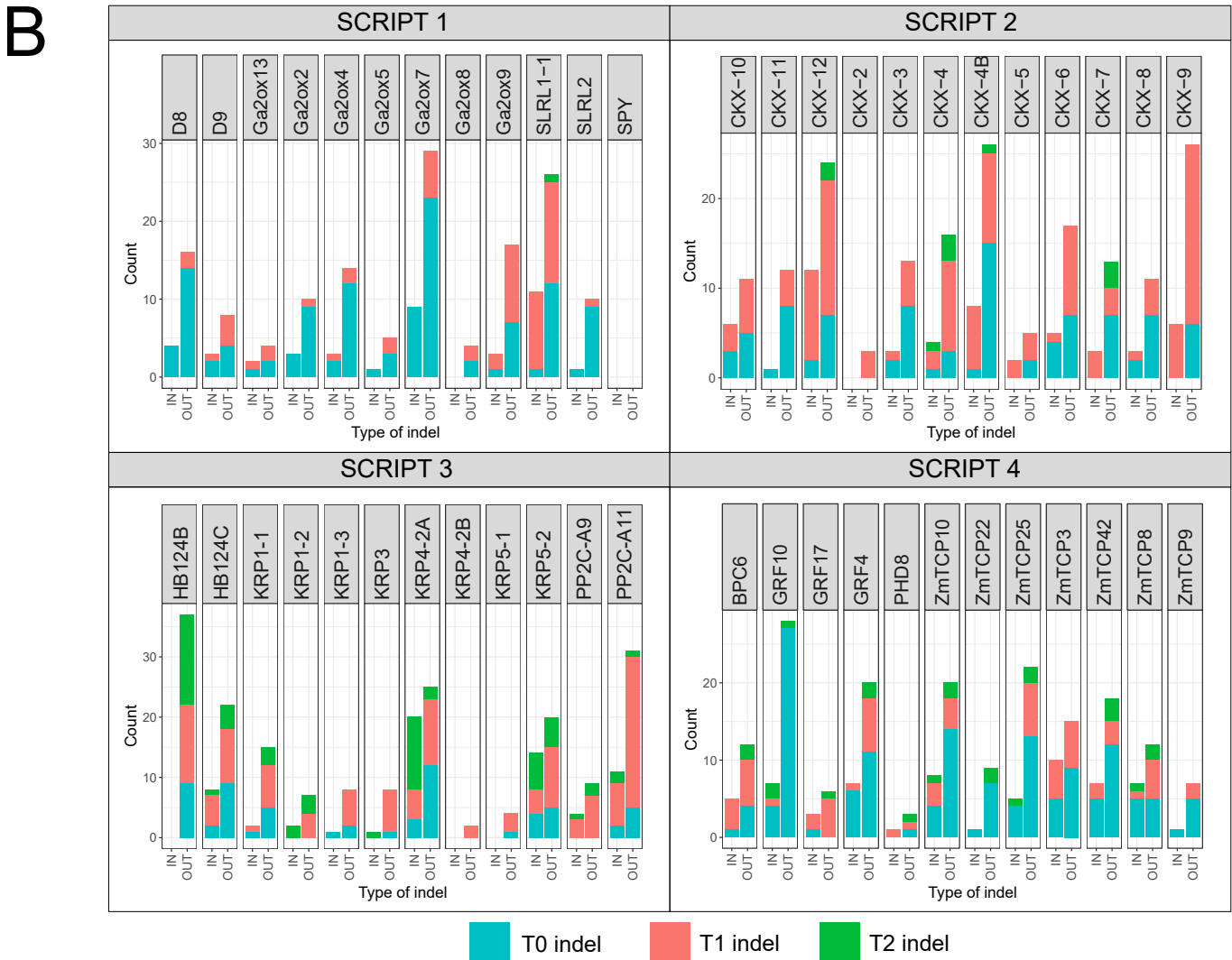
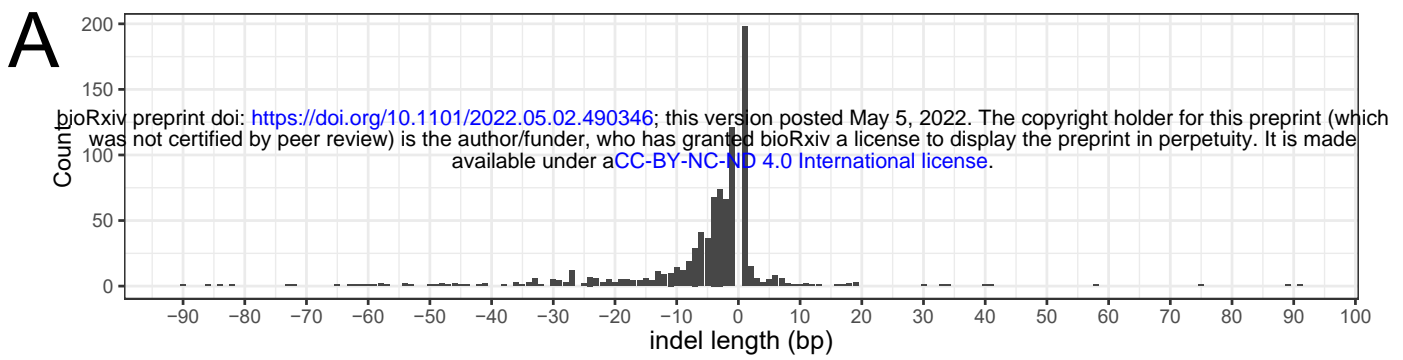


Figure 2. Diversity of mutated haplotypes obtained after CRISPR/Cas9 genome editing. **A**. Distribution of indel length. **B**. Number of different haplotypes with indels observed per gene. Any haplotype with indels with >1% relative frequency in the sequencing reads per locus per sample is included. IN: in-frame indel, OUT: out-frame indel. Blue, red, and green correspond to fractions of indels first observed at T0, T1, and T2, respectively. **C**. Different haplotype combinations in plants can all lead to a gene loss-of-function, either partial (LOF_{1/2}) or complete (LOF_{2/2}). Each colored horizontal stacked bar corresponds to a different haplotype_{KO}. Bar length is proportional to the fraction of sequencing reads per locus containing the haplotype_{KO}. The black fraction corresponds to the aggregation of alleles assigned to the wild-type haplotype (haplotype_{REF}). For an overview of the different haplotype_{KO} found in T0 plants harboring the different SCRIPTs, see Supplemental Figure S5.

A

■ LOF_{0/2}
■ LOF_{1/2}
■ LOF_{2/2}
 NA

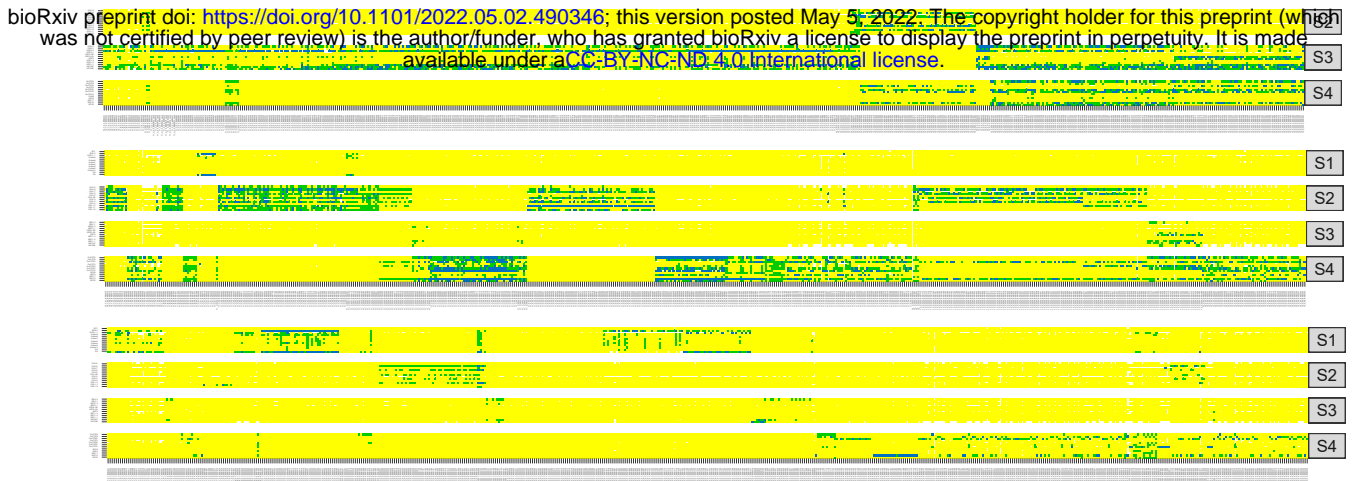
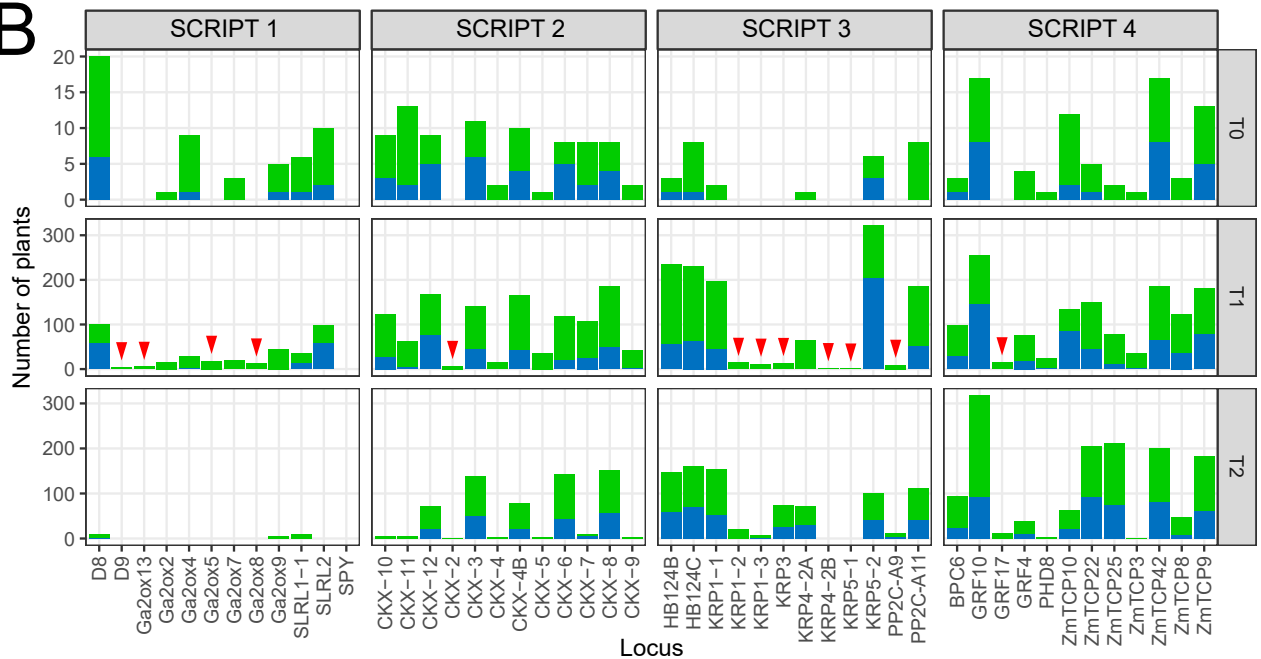
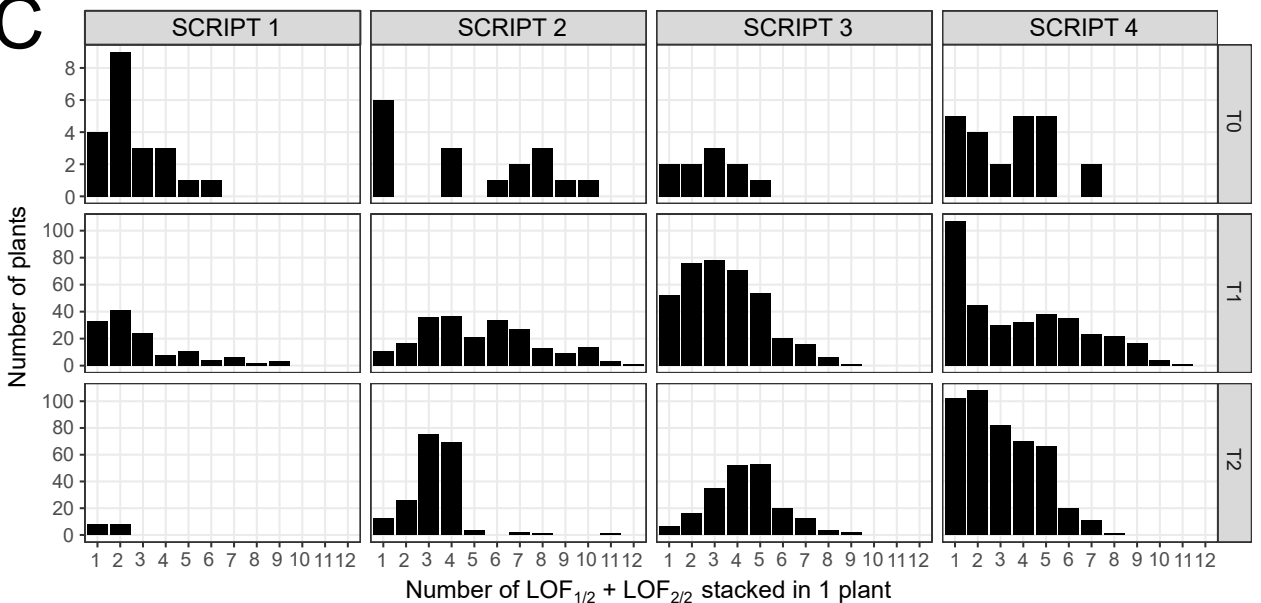
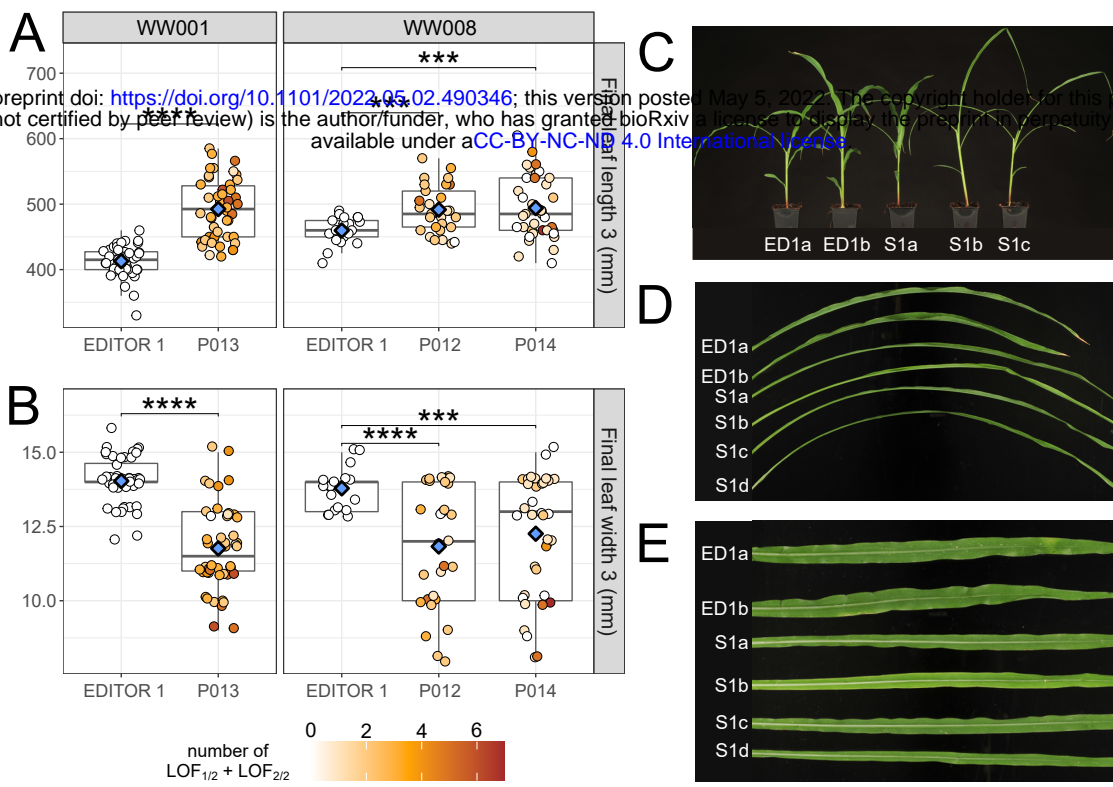
**B****C**

Figure 3. Distribution of LOF in genes across the entire set of samples. Only haplotype_{KO} were considered for genotype calling. The fractions of reads containing haplotype_{KO} were summed per sample per locus. **A.** Overview of the classes LOF_{0/2}, LOF_{1/2}, or LOF_{2/2} obtained in the entire sample set for the four SCRIPTS (S1-S4). Samples are on the x-axis and distributed over three rows. **B.** Distributions of LOF_{1/2} (green) and LOF_{2/2} (blue) across the four SCRIPTS throughout generations. The top, middle, and bottom panels show T0, T1, and T2 plants, respectively. Red triangles indicate new LOF that appeared at T1. **C.** Stacking LOF at multiple genes within plants.

SCRIPT 1



SCRIPT 4

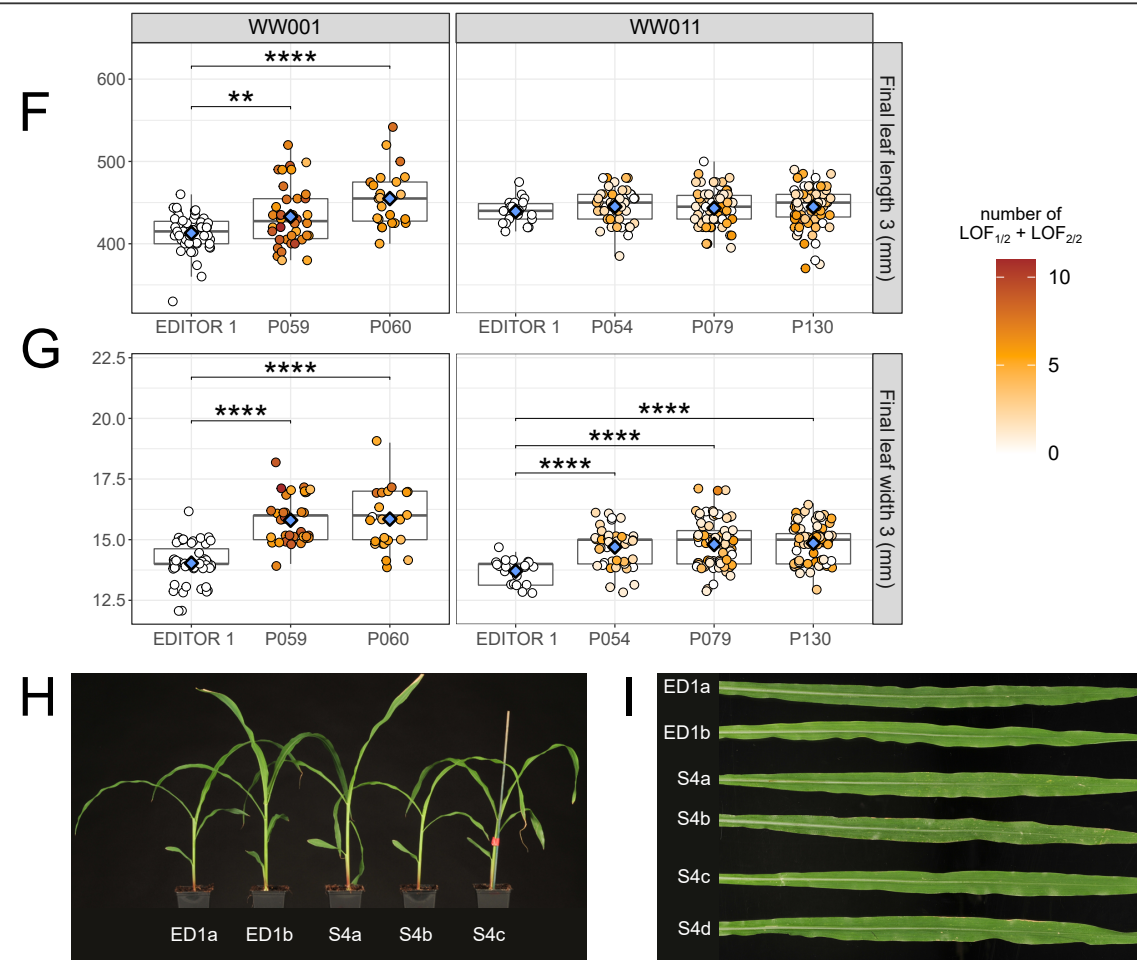


Figure 4. Phenotypes observed in multiple gene-edited populations of SCRIPT 1 and SCRIPT 4. A-B, F-G. Measurements of final length of leaf 3 (FLL3) (A, F) and final leaf width (FLW3) (B, G) of gene-edited SCRIPT 1 (A, B) and SCRIPT 4 (F, G) individuals compared with the EDITOR 1 background control. For each SCRIPT, data corresponds to independent multiple gene-edited populations assayed on two different independent experiments under WW conditions. On the distributions, each dot represents one individual and is colored according to the amount of partial ($LOF_{1/2}$) and complete ($LOF_{2/2}$) LOF observed in that individual. The more orange, the higher the LOF in the individual. Pairwise Student's t-test were conducted between EDITOR 1 and mutated populations. Significant differences are displayed with p-values summarized as follow: ** = $p < 0.01$, *** = $p < 1e-3$, **** = $p < 1e-4$. Blue diamonds indicate the mean of each distribution. C-D, H-I. Pictures of general plant architecture (C for SCRIPT 1 and H for SCRIPT 4) and final leaf 3 (D for SCRIPT 1 and I for SCRIPT 4) compared with the EDITOR 1 (ED1) background.

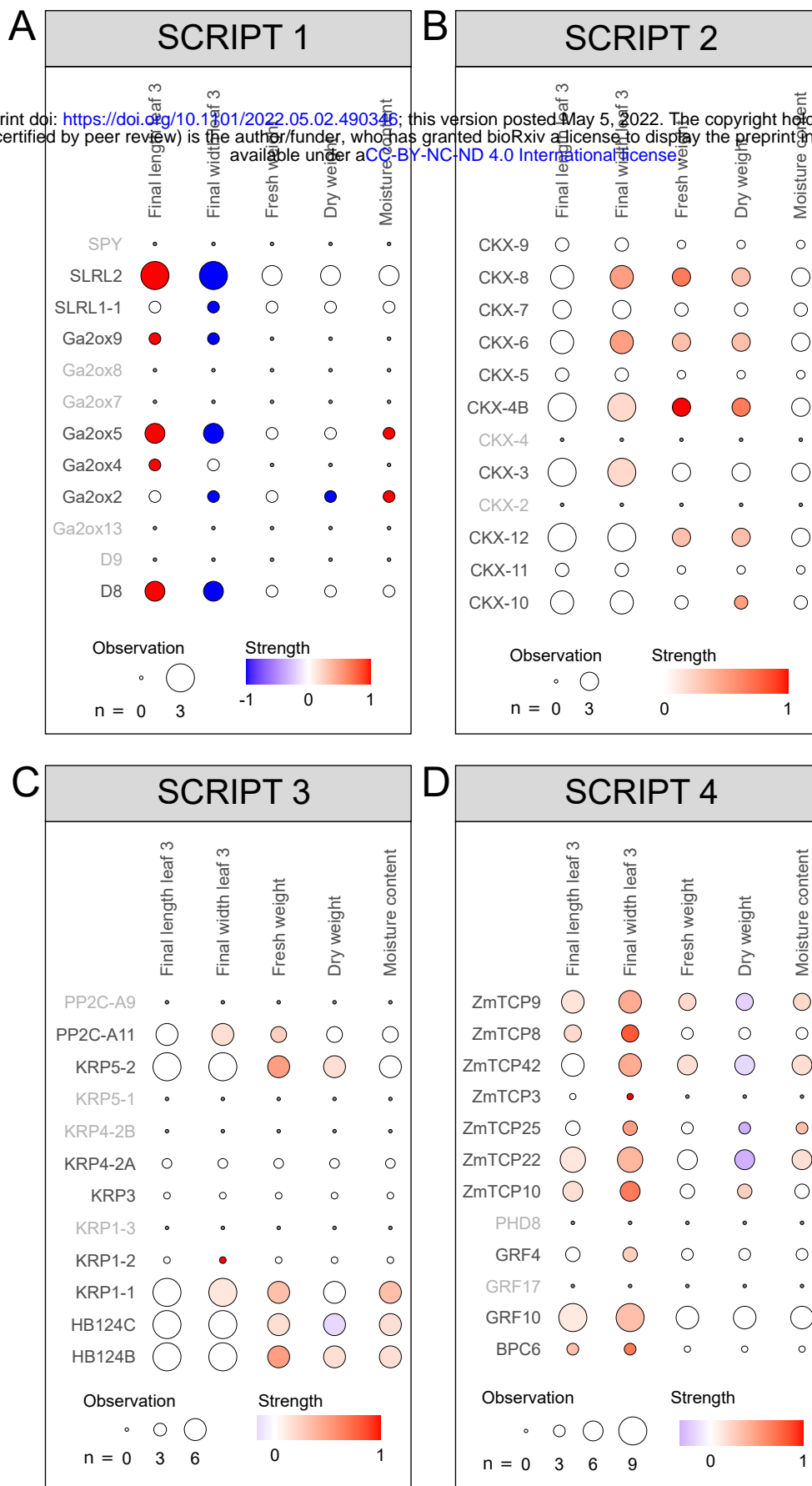


Figure 5. Aggregated association analysis of single-gene LOF and traits. Summaries of single-gene associations to traits are represented for SCRIPT 1 (A), SCRIPT 2 (B), SCRIPT 3 (C), and SCRIPT 4 (D). Single-gene associations were performed per population, in each phenotypic experiment and for all measured traits. Results are summarized per gene, per trait with two indices. 1) Observation: the number of time a given gene has been observed in a situation with sufficient genotypic and phenotypic data across populations and experiments. An observation with sufficient data corresponds to a situation where a gene displays at least one LOF group between LOF_{1/2} and LOF_{2/2} represented by at least six individuals with phenotypic information for a specific trait. In such cases, the mean phenotypic value of each genotypic group could be statistically compared to the mean phenotypic value of the EDITOR 1 control. 2) Strength: for each gene, we calculated the weighted sum of observations in which the genotypic group with the highest mean phenotypic value is above (weight: +1) or below (weight: -1) 10% the mean phenotypic value of EDITOR 1. The resulting sum was divided by the total number of observations (n). Associations displaying highest strength, either positive or negative, along with a large total number of observations indicate strong evidence for a gene effect on the trait.

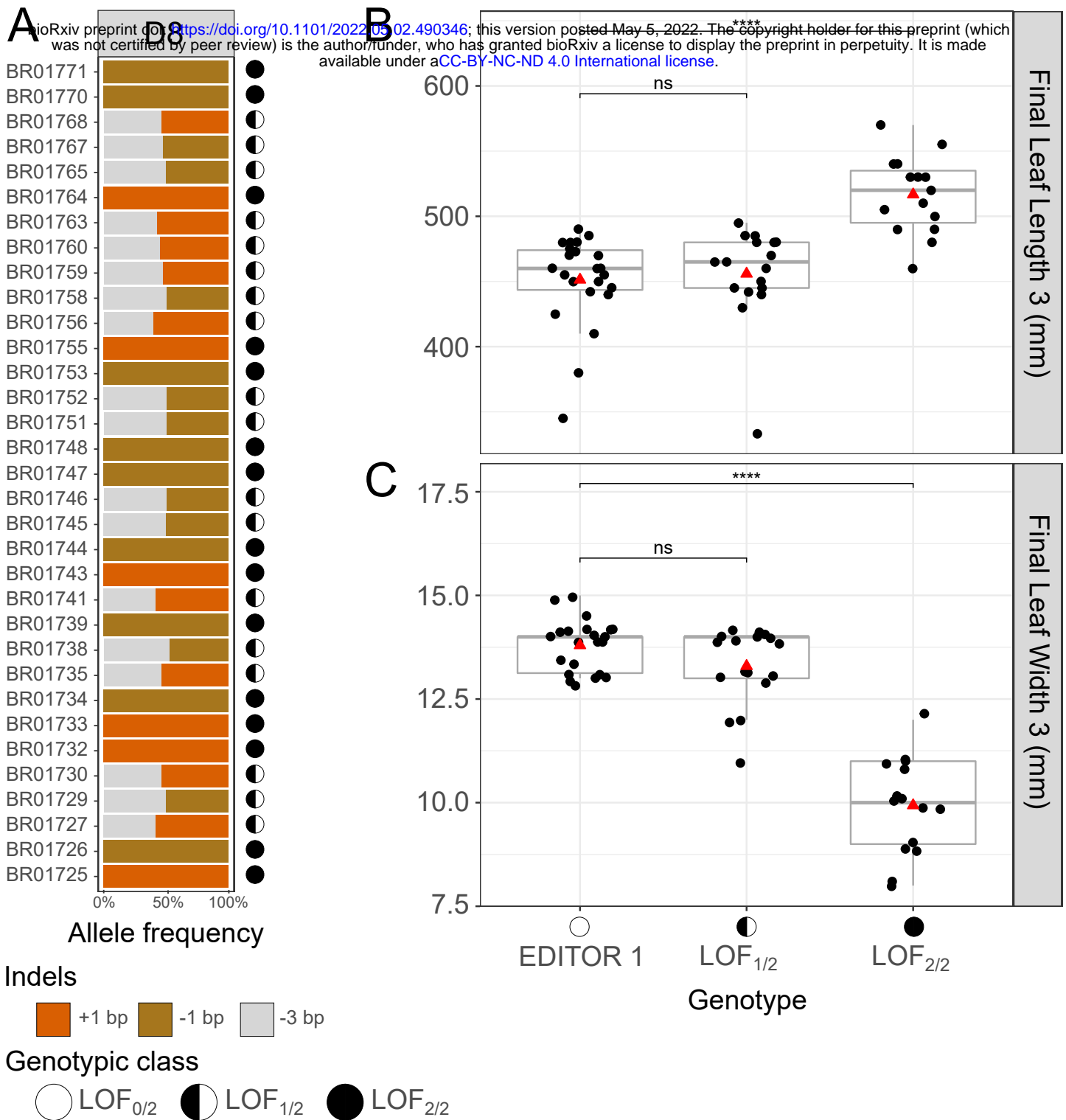


Figure 6. LOF dosages in *D8* and leaf shape parameters. **A**. Haplotype profiles at gene *D8* of T1 segregants from population P012. Three haplotypes were detected, with two containing out-frame indels (-1 bp, brown and +1 bp, orange) and one containing an in-frame (-3 bp, gray) deletion. This results in a collection of plants with *D8* either partially (LOF_{1/2}) or completely (LOF_{2/2}) knocked out. The resulting two classes of LOF dosages are compared to EDITOR 1 for final leaf length 3 (**B**) and final leaf width 3 (**C**). Significant differences (pairwise Student's *t*-test) are displayed with p-values summarized as follow: *** = $p < 1e-3$, ns: not-significant. Red triangles indicate the mean of each distribution.

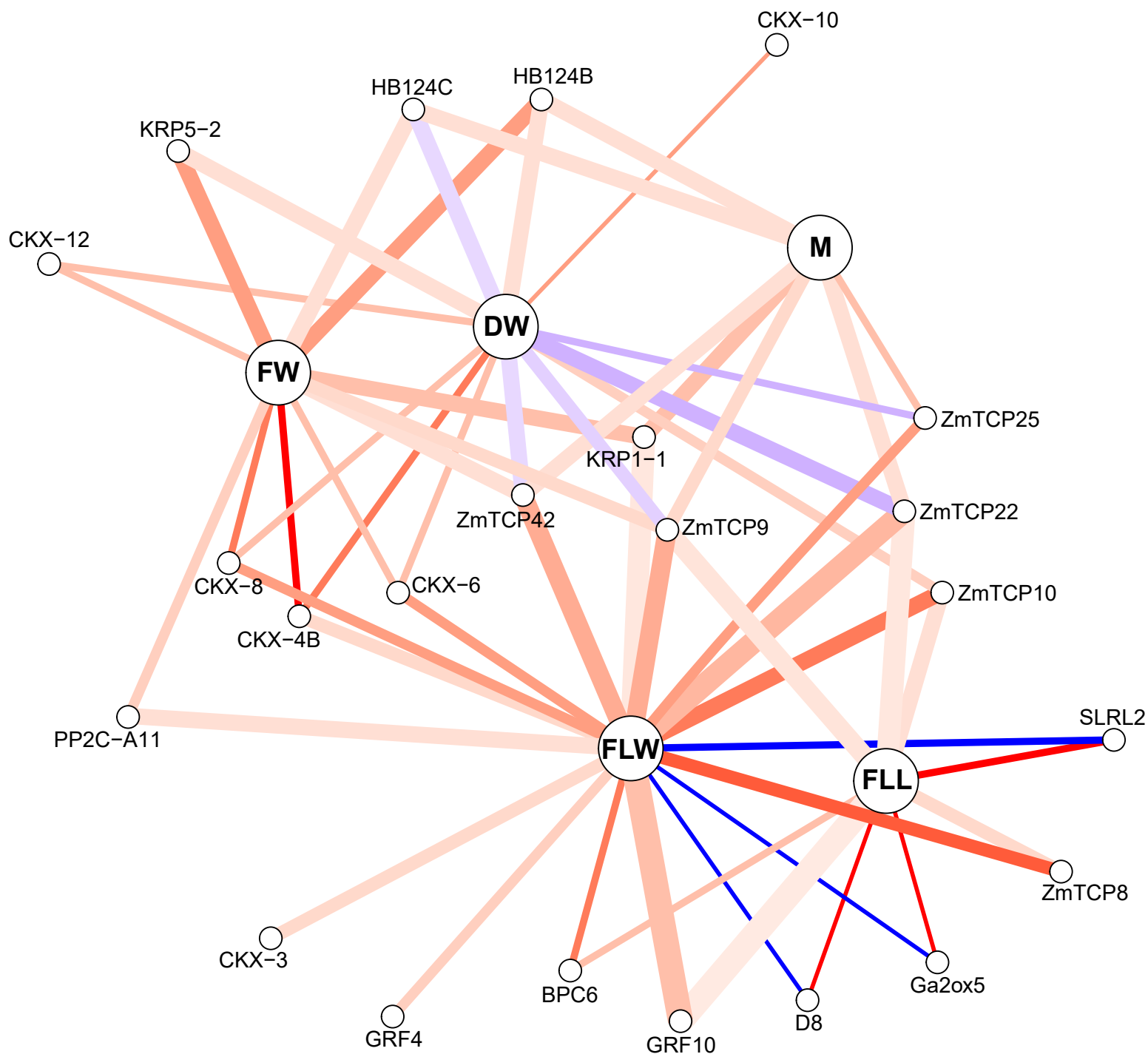


Figure 7. Network representation of single-gene effects on growth-related traits. Traits are displayed in bold (FLL: final leaf length; FLW: final leaf width; FW: fresh weight; DW: dry weight; M: moisture content). Genes at least associated once with a trait are displayed. Lines indicate connections between genes and traits. Line width is proportional to the number of times the underlying dataset to detect a gene knockout-trait association in different experiments and/or populations contained sufficient data for statistics (i.e., minimum one LOF class between $LOF_{1/2}$ and $LOF_{2/2}$ with at least six individuals with phenotypic information). Line color represents the weighted fraction of gene KO-trait associations that significantly outperformed by 10% the EDITOR 1 control (ANOVA test; $p < 5\%$), either positively (weight: +1, more red) or negatively (weight: -1, more blue), over the number of times a gene KO-trait association could have been observed because of sufficient data points.

ID population	Scripts	Generation	Type	Total edited loci	Fixed loci	Experiment
P012	S1	T1	Self	9/12	1	WW08
P013	S1	T1	Intrascript	11/12	2	WW01
P014	S1	T1	Self	9/12	1	WW08
P019	S2	T1	Self	10/12	2	WW01, WD03
P108	S2	T1	Intrascript	11/12	0	WW01, WD05
P032	S3	T1	Self	6/12	0	WW1
P033	S3	T1	Self	7/12	1	WW1, WD07
P034	S3	T1	Intrascript	10/12	1	WD07
P030	S3	T1	Self	5/12	0	WD07
P059	S4	T1	Intrascript	12/12	5	WW01
P060	S4	T1	Self	9/12	5	WW01
P054	S4	T1	Self	9/12	0	WW11
P079	S4	T1	Self	10/12	0	WW11
P130	S4	T2	Self	11/12	0	WW11
P148	S2 + S4	T2	Interscript	7/24	0	WD09
P152	S2 + S4	T2	Interscript	8/24	0	WD09
P157	S3 + S4	T2	Interscript	16/24	0	WD06
P158	S3 + S4	T2	Interscript	16/24	0	WD06

Supplemental Table 1: Detailed information of populations used in the phenotyping assays. The number of loci edited correspond to segregating or fixed loci with an aggregated ratio of indels of 40% in at least 3 plants in the population.

Script	Position	Gene	gRNA	Amplicon primer Fw	Amplicon Primer Rv
1	1	<i>ZmGa2ox2</i>	TATATGCAGGGACGTGGTGCAGG	GGCCTAAAACCAGAGCTGC	CCTCGTCGTGGCCAGAAG
1	2	<i>ZmGa2ox4</i>	GGCGCGATGTCAAAGCTGGCCGG	ACATATCGGTGCAGCAGGG	GTCTCGTCGCACCCCTCC
1	3	<i>ZmGa2ox5</i>	CGGACGGGTGACCCGGCACCTGG	AACGACGTGGACGGCCTG	ATCTCACCGACCTGAAGGGC
1	4	<i>ZmGa2ox7</i>	TGACGGGACAGGGGAGGCCTTGG	CGACATGGGGTGGCTCGA	TTCGCTGACACTGCATGCAT
1	5	<i>ZmGa2ox8</i>	CGACGAGATCTTACGGTGTGG	GGTACGGCAGCAAGAGCATC	CGAAGACGAGGCAACAACAA
1	6	<i>ZmGa2ox9</i>	CCGCGCCGGCCGGCCGTTACGG	CATTATTGCCCTGCGCCG	GACTCAGGAGGCAAGCGAAG
1	7	<i>ZmGa2ox13</i>	AGGCAGGGGTAGTTCAGCGCCGG	GCGGACAGCGACTGCATG	GGAGCACCGAGATGATCTGC
1	8	<i>D8</i>	TCGAGGAGGGAGCTGTCCGGTGG	GCAAGGTCGCCGCTACT	GTAGGGGCAGGACTCGTAGA
1	9	<i>D9</i>	GGAGGGAGCCGTCCGGTCCGGG	GCAAGGTCGCCGCTACT	GTAGGGGCAGGACTCGTAGA
1	10	<i>ZmSLRL1-1</i>	ACGGCGGCCCAATGCCCGTGAGG	CTGATCCAGGCCCTCGCG	GGAGAAGTGGACGCGCAC
1	11	<i>ZmSLRL2</i>	GTACACCTCTGTGAGTGAGTCGG	ATGCCCTTTCCACTATGCG	TCGCCGACACAATGTCAAA
1	12	<i>ZmSPY</i>	GATAACTCCCATGTTGCAATAGG	TGTTACGAGAAAAGCTGCACT	AGCATACCTCTCGTAGCAGA
2	1	<i>ZmCKX-2</i>	ATAGCACTCTTCCATCTGACTGG	CAGGACAGGCATCCTCAACA	CCATGGTATCAGTGTGCCA
2	2	<i>ZmCKX-3</i>	TGAGACGCTCAAGCACGGTCTGG	CCCGGAGGAGAGCTCTGGATCA	GACATTGCTGACCTGCGGTCCG
2	3	<i>ZmCKX-4</i>	CTTGAGCGAGGTGAGCTTACGG	GGGCCTCATCAACAAGTGA	CTGCGGTTTCGTCGTCGTAG
2	4	<i>ZmCKX-4B</i>	TGTTGTGGCTGTTACCTTTGGG	AACCCGGACCTATTCTTCGG	GGGAGAGACAGGAGGGAGAG
2	5	<i>ZmCKX-5</i>	TTCTGGACCGCGTGAGCGCCGG	GACGTGATGCTGCGTGAG	GAGGTTGAGCCACGGGTG
2	6	<i>ZmCKX-6</i>	CTTCGAGACGGGTGAGGATGG	CTGGAGGCATCTCGAG	GTGCACCTCCTCCACATC
2	7	<i>ZmCKX-7</i>	TTCTATGTCAGCTTACGGGGG	SAACAATGCAGGCACAGGTG	CTCAAGCCGGATCCGTGC
2	8	<i>ZmCKX-8</i>	GAACCTCGACCTGTTTCATGGCGG	GAACAATGCAGGCACAGGTG	CTCAAGCCGGATCCGTGC
2	9	<i>ZmCKX-9</i>	CACCCAATGCTGCGTAGAACAGG	TGTGTGATCGAGCTGTGTTT	GTTCAAGCGGATCCGAG
2	10	<i>ZmCKX-10</i>	AGGCCCGCACGTGCTTGAAGCGG	CGTTGGTTATGGTTCGTGCG	TCCTCCTCCACCCGGTTC
2	11	<i>ZmCKX-11</i>	TCCTCTGCAGTTGTGGACCTGG	GAAGGGCCATTGTTGACGAC	CCGCACCCAGTTGAGGAAAT
2	12	<i>ZmCKX-12</i>	TTGGGCGGAGCAACTGCAGCGG	TTCTTCGCCGTAATTGGTGG	ACCAGCTAGAGAGGAAGCAG
3	1	<i>ZmKRP1;1</i>	CTCGCGTCTGGGCCGCTCCCGG	CTACGACGTAACAGGCTGGC	TTCAGCAGGAATCGCGAGAC
3	2	<i>ZmKRP1;2</i>	TGTGTCACCCGCGAGCAACTCGG	ATTGTGCGGGCTCTAACTCT	ACGGTGGGAGGCATAATTCA
3	3	<i>ZmKRP1;3</i>	CGCAGAAGCTGTGCTCGCGACGG	CAACGTGGGGAGGACGAC	GTGTTCCAGTCACTGCCG
3	4	<i>ZmKRP3</i>	CTTACGCTCTGCGAATCGCCGG	GGAAACCGAGATAGAGGCCT	CACCACGCCAACCCAACT
3	5	<i>ZmKRP4;2A</i>	CTCCTCACGGACGCCACCTGCGG	GCGAGTACCTGGAGCTAAGG	CATGTTCTCCCCGTACGACG
3	6	<i>ZmKRP4;2B</i>	CCCGACCTCCTCGTGGTCCCGG	GCGAGTACCTGGAGCTAAGG	CATGTTCTCCCCGTACGACG
3	7	<i>ZmKRP5;1</i>	CCGCACGCTCGGCTGCAGAGGG	GTGGCCGTCATGGAGGTC	TCCTGAGCTCGAGGTACTGT
3	8	<i>ZmKRP5;2</i>	CGGTATGAACCGGCAGCTCGGGG	CCCAGAGATGATAAGCACCCC	GAACTCCTCCATCTCGAGCG
3	9	<i>ZmPP2C-A9</i>	GGCTCGCCATGCACTTCTTCGG	CTCGCTCCATCCGGACTTG	GACTAGCTGGAGATTGGCGG
3	10	<i>ZmPP2C-A11</i>	GACACTCGTGCCAGAACCTGTGG	GGAGGTGGTGAAGAAGCAGG	GCCCGTGAATCTCCACAGTT
3	11	<i>ZmHB124B</i>	CATGGAGGATATCCACGCACCCGG	ACTAGTCCATAGGTGCGGGA	ACCTGCATGTAGATAAGCTCGA
3	12	<i>ZmHB124C</i>	AGGTCATTGACTCAGTCCACTGG	TTTTGCTTGATCATTATTTGATGCA	GGAAGCACCTCAGCTCTGAT
4	1	<i>ZmTCP3</i>	AGGCGCGCACGGGCTGTGACGG	ATCAGCAGCCCAACGTCTC	CCGAACGGAGGCGCATTG
4	2	<i>ZmTCP8</i>	CAGCACTTCGGCTTGCCAGTGG	GCTCCTCACCTCGGCAAC	GCAAGAACGAGAAGTGCCTC
4	3	<i>ZmTCP9</i>	CAGCTCCTGGCTGTGTCGCCGG	CAGTCGTCGACCATGGGG	GACCGGTGGTGGAAACATGG
4	4	<i>ZmTCP10</i>	TGCCCAACCATGAGGTCTGCGG	TCAACCAGCCTAGCAAGGTC	TTCTCGTCGTGACCATCAG
4	5	<i>ZmTCP22</i>	CCAGTTCGCCCGCAAGGGCAGG	GAGCAAGGTGGTGGACTGG	CTGCAACGTTGGCAAAGGG
4	6	<i>ZmTCP25</i>	GTACCGGTCCAAGACTCGCCGGG	AATTCCATCCGCTCGTCAA	GAGATGAGAAGGGCGAGTGG
4	7	<i>ZmTCP42</i>	CTCGAAGGATATGGCCGACGCGG	CGCCAACAACAGCAGCAAG	GGCTGCTCCTGAAGGAAGG
4	8	<i>ZmGRF4</i>	CATCCGTCCCTGACGGTGTGGG	CTGGTTACAGCTGCAGCAAC	TGATAAACCCGGGACTGCTG
4	9	<i>ZmGRF10</i>	GGACCTCCGATCCTCGACCAGG	GACAAGGCGGATCGAGAGG	GAGAGAGTCAGCCAGAACGG
4	10	<i>ZmGRF17</i>	TTCTGTCTGTTGCGAGGAGAGG	CTGATCGCTCTGTGTTGGC	GGACACATCCGCTCTCG
4	11	<i>ZmPHD8</i>	CACTGGACATATGAACAAACCGG	AGTGGAACAGGAAAAATGGGGT	TCTGTCTGTTTACTAGCTTCTCA
4	12	<i>ZmBPC6</i>	TTCTTTGTTCCATTGAGAGGAGG	CCTAGCTGCACTCGAACTC	GCGGGGATGTTTGGACATGA

Supplemental Table 2: List of gRNAs and associated primer pairs for edit detection using HiPlex amplicon sequencing.

Full name	type	Cloning sites	Bacterial Selection	Plant Selection
pGG-A-OsU3-BbsI-ccdB-BbsI-B	Entry vector	A-B	Ampicilin	
pGG-B-OsU3-BbsI-ccdB-BbsI-C	Entry vector	B-C	Ampicilin	
pGG-C-OsU3-BbsI-ccdB-BbsI-D	Entry vector	C-D	Ampicilin	
pGG-D-OsU3-BbsI-ccdB-BbsI-E	Entry vector	D-E	Ampicilin	
pGG-E-OsU3-BbsI-ccdB-BbsI-F	Entry vector	E-F	Ampicilin	
pGG-F-OsU3-BbsI-ccdB-BbsI-G	Entry vector	F-G	Ampicilin	
pGG-B-U1-OsU3-BbsI-ccdB-BbsI-C	Entry vector with U-linker	B-C	Ampicilin	
pGG-C-U2-OsU3-BbsI-ccdB-BbsI-D	Entry vector with U-linker	C-D	Ampicilin	
pGG-D-U3-OsU3-BbsI-ccdB-BbsI-E	Entry vector with U-linker	D-E	Ampicilin	
pGG-E-U4-OsU3-BbsI-ccdB-BbsI-F	Entry vector with U-linker	E-F	Ampicilin	
pGG-F-U5-OsU3-BbsI-ccdB-BbsI-G	Entry vector with U-linker	F-G	Ampicilin	
pEN-2xTaU3	PCR template		Kanamycin	
pGG-A-Script1-entry1-B	Paired gRNA entry vector	A-B	Ampicilin	
pGG-B-Script1-entry2-C	Paired gRNA entry vector	B-C	Ampicilin	
pGG-C-Script1-entry3-D	Paired gRNA entry vector	C-D	Ampicilin	
pGG-D-Script1-entry4-E	Paired gRNA entry vector	D-E	Ampicilin	
pGG-E-Script1-entry5-F	Paired gRNA entry vector	E-F	Ampicilin	
pGG-F-Script1-entry6-G	Paired gRNA entry vector	F-G	Ampicilin	
pGG-A-Script2-entry1-B	Paired gRNA entry vector	A-B	Ampicilin	
pGG-B-Script2-entry2-C	Paired gRNA entry vector	B-C	Ampicilin	
pGG-C-Script2-entry3-D	Paired gRNA entry vector	C-D	Ampicilin	
pGG-D-Script2-entry4-E	Paired gRNA entry vector	D-E	Ampicilin	
pGG-E-Script2-entry5-F	Paired gRNA entry vector	E-F	Ampicilin	
pGG-F-Script2-entry6-G	Paired gRNA entry vector	F-G	Ampicilin	
pGG-A-Script3-entry1-B	Paired gRNA entry vector	A-B	Ampicilin	
pGG-B-Script3-entry2-C	Paired gRNA entry vector	B-C	Ampicilin	
pGG-C-Script3-entry3-D	Paired gRNA entry vector	C-D	Ampicilin	
pGG-D-Script3-entry4-E	Paired gRNA entry vector	D-E	Ampicilin	
pGG-E-Script3-entry5-F	Paired gRNA entry vector	E-F	Ampicilin	
pGG-F-Script3-entry6-G	Paired gRNA entry vector	F-G	Ampicilin	
pGG-A-Script4-entry1-B	Paired gRNA entry vector	A-B	Ampicilin	
pGG-B-Script4-entry2-C	Paired gRNA entry vector	B-C	Ampicilin	
pGG-C-Script4-entry3-D	Paired gRNA entry vector	C-D	Ampicilin	
pGG-D-Script4-entry4-E	Paired gRNA entry vector	D-E	Ampicilin	
pGG-E-Script4-entry5-F	Paired gRNA entry vector	E-F	Ampicilin	
pGG-F-Script4-entry6-G	Paired gRNA entry vector	F-G	Ampicilin	
pGG-A-Script5-entry1-B	Paired gRNA entry vector	A-B	Ampicilin	
pGG-B-Script5-entry2-C	Paired gRNA entry vector	B-C	Ampicilin	
pGG-C-Script5-entry3-D	Paired gRNA entry vector	C-D	Ampicilin	
pGG-D-Script5-entry4-E	Paired gRNA entry vector	D-E	Ampicilin	
pGG-E-Script5-entry5-F	Paired gRNA entry vector	E-F	Ampicilin	
pGG-F-Script5-entry6-G	Paired gRNA entry vector	F-G	Ampicilin	
pGGBb-AG	Destination vector	A-G	Spectinomycin	Bar
pGG-AG-Script1	Expression vector	A-G	Spectinomycin	Bar
pGG-AG-Script2	Expression vector	A-G	Spectinomycin	Bar
pGG-AG-Script3	Expression vector	A-G	Spectinomycin	Bar
pGG-AG-Script4	Expression vector	A-G	Spectinomycin	Bar
pGG-AG-Script5	Expression vector	A-G	Spectinomycin	Bar

Supplemental Table 3: Plasmid overview.

bioRxiv preprint doi: <https://doi.org/10.1101/2022.05.02.490346>; this version posted May 5, 2022. The copyright holder for this preprint (which was not certified by peer review) is the author/funder, who has granted bioRxiv a license to display the preprint in perpetuity. It is made available under a [CC-BY-NC-ND 4.0 International license](https://creativecommons.org/licenses/by-nc-nd/4.0/).

Parsed Citations

- Anzalone AV, Koblan LW, and Liu DR. (2020).** Genome editing with CRISPR-Cas nucleases, base editors, transposases and prime editors. *Nat. Biotechnol.* 38: 824-844
Google Scholar: [Author Only](#) [Title Only](#) [Author and Title](#)
- Ashikari M, Sakakibara H, Lin S, Yamamoto T, Takashi T, Nishimura A, Angeles ER, Qian Q, Kitano H, and Matsuoka M. (2005).** Cytokinin oxidase regulates rice grain production. *Science* 309: 741-745
Google Scholar: [Author Only](#) [Title Only](#) [Author and Title](#)
- Bai M, Yuan J, Kuang H, Gong P, Li S, Zhang Z, Liu B, Sun J, Yang M, Yang L, et al. (2020).** Generation of a multiplex mutagenesis population via pooled CRISPR-Cas9 in soya bean. *Plant Biotechnol. J.* 18: 721-731
Google Scholar: [Author Only](#) [Title Only](#) [Author and Title](#)
- Bartrina I, Otto E, Strnad M, Werner T, and Schmülling T. (2011).** Cytokinin regulates the activity of reproductive meristems, flower organ size, ovule formation, and thus seed yield in *Arabidopsis thaliana*. *Plant Cell* 23: 69-80
Google Scholar: [Author Only](#) [Title Only](#) [Author and Title](#)
- Baute J, Herman D, Coppens F, De Block J, Slabbinck B, Dell'Acqua M, Pè ME, Maere S, Nelissen H, and Inzé D. (2015).** Correlation analysis of the transcriptome of growing leaves with mature leaf parameters in a maize RIL population. *Genome Biol.* 16: 168
Google Scholar: [Author Only](#) [Title Only](#) [Author and Title](#)
- Baute J, Herman D, Coppens F, De Block J, Slabbinck B, Dell'Acqua M, Pè ME, Maere S, Nelissen H, and Inzé D. (2016).** Combined large-scale phenotyping and transcriptomics in maize reveals a robust growth regulatory network. *Plant Physiol.* 170: 1848-1867
Google Scholar: [Author Only](#) [Title Only](#) [Author and Title](#)
- Berendzen K, Searle I, Ravenscroft D, Koncz C, Batschauer A, Coupland G, Somssich IE, and Ülker B. (2005).** A rapid and versatile combined DNA/RNA extraction protocol and its application to the analysis of a novel DNA marker set polymorphic between *Arabidopsis thaliana* ecotypes Col-0 and Landsberg erecta. *Plant Methods* 1: 4
Google Scholar: [Author Only](#) [Title Only](#) [Author and Title](#)
- Bhat JA, Yu D, Bohra A, Ganie SA, and Varshney RK. (2021).** Features and applications of haplotypes in crop breeding. *Commun. Biol.* 4: 1266
Google Scholar: [Author Only](#) [Title Only](#) [Author and Title](#)
- Bloch D, Puli MR, Mosquna A, and Yalovsky S. (2019).** Abiotic stress modulates root patterning via ABA-regulated microRNA expression in the endodermis initials. *Development* 146: dev177097
Google Scholar: [Author Only](#) [Title Only](#) [Author and Title](#)
- Borg M, and Berger F. (2015).** Chromatin remodelling during male gametophyte development. *Plant J.* 83: 177-188
Google Scholar: [Author Only](#) [Title Only](#) [Author and Title](#)
- Brás TA, Seixas J, Carvalhais N, and Jägermeyr J. (2021).** Severity of drought and heatwave crop losses tripled over the last five decades in Europe. *Environ. Res. Lett.* 16: 065012
Google Scholar: [Author Only](#) [Title Only](#) [Author and Title](#)
- Cao L, Wang S, Venglat P, Zhao L, Cheng Y, Ye S, Qin Y, Datla R, Zhou Y, and Wang H. (2018).** *Arabidopsis* ICK/KRP cyclin-dependent kinase inhibitors function to ensure the formation of one megaspore mother cell and one functional megaspore per ovule. *PLoS Genet.* 14: e1007230
Google Scholar: [Author Only](#) [Title Only](#) [Author and Title](#)
- Chaikam V, Molenaar W, Melchinger AE, and Boddupalli PM. (2019).** Doubled haploid technology for line development in maize: technical advances and prospects. *Theor. Appl. Genet.* 132: 3227-3243
Google Scholar: [Author Only](#) [Title Only](#) [Author and Title](#)
- Cheng Y, Cao L, Wang S, Li Y, Shi X, Liu H, Li L, Zhang Z, Fowke LC, Wang H, et al. (2013).** Downregulation of multiple CDK inhibitor ICK/KRP genes upregulates the E2F pathway and increases cell proliferation, and organ and seed sizes in *Arabidopsis*. *Plant J.* 75: 642-655
Google Scholar: [Author Only](#) [Title Only](#) [Author and Title](#)
- Colombo N, and Favret EA (1996).** The effect of gibberellic acid on male fertility in bread wheat. *Euphytica* 91: 297-303
Google Scholar: [Author Only](#) [Title Only](#) [Author and Title](#)
- Coussens G, Aesaert S, Verelst W, Demeulenaere M, De Buck S, Njuguna E, Inzé D, and Van Lijsebettens M. (2012).** *Brachypodium distachyon* promoters as efficient building blocks for transgenic research in maize. *J. Exp. Bot.* 63: 4263-4273
Google Scholar: [Author Only](#) [Title Only](#) [Author and Title](#)
- Czesnick H, and Lenhard M. (2015).** Size control in plants-lessons from leaves and flowers. *Cold Spring Harb. Perspect. Biol.* 7:

a019190

Google Scholar: [Author Only](#) [Title Only](#) [Author and Title](#)

Decaestecker W, Andrade Buono R, Pfeiffer ML, Vangheluwe N, Jourquin J, Karimi M, Van Isterdael G, Beeckman T, Nowack MK, and Jacobs TB. (2019). CRISPR-TSKO: a technique for efficient mutagenesis in specific cell types, tissues, or organs in Arabidopsis. Plant Cell 31: 2868-2887

Google Scholar: [Author Only](#) [Title Only](#) [Author and Title](#)

Doll NM, Gilles LM, Gerentes M-F, Richard C, Just J, Fierlej Y, Borrelli VMG, Gendrot G, Ingram GC, Rogowsky PM, et al. (2019). Single and multiple gene knockouts by CRISPR-Cas9 in maize. Plant Cell Rep. 38: 487-501

Google Scholar: [Author Only](#) [Title Only](#) [Author and Title](#)

Elias F, Muleta D, and Woyessa D. (2016). Effects of phosphate solubilizing fungi on growth and yield of haricot bean (*Phaseolus vulgaris* L.) plants. J. Agric. Sci. 8: 204-218

Google Scholar: [Author Only](#) [Title Only](#) [Author and Title](#)

Gaillochet C, Develtere W, and Jacobs TB. (2021). CRISPR screens in plants: approaches, guidelines, and future prospects. Plant Cell 33: 794-813

Google Scholar: [Author Only](#) [Title Only](#) [Author and Title](#)

Gong P, Bontinck M, Demuyne K, De Block J, Gevaert K, Eeckhout D, Persiau G, Aesaert S, Coussens G, Van Lijsebettens M, et al. (2022). SAMBA controls cell division rate during maize development. Plant Physiol. 188: 411-424

Google Scholar: [Author Only](#) [Title Only](#) [Author and Title](#)

Gong R, Cao H, Zhang J, Xie K, Wang D, and Yu S. (2018). Divergent functions of the GAGA-binding transcription factor family in rice. Plant J. 94: 32-47

Google Scholar: [Author Only](#) [Title Only](#) [Author and Title](#)

Gonzalez N, Vanhaeren H, and Inzé D. (2012). Leaf size control: complex coordination of cell division and expansion. Trends Plant Sci. 17: 332-340

Google Scholar: [Author Only](#) [Title Only](#) [Author and Title](#)

Hai NN, Chuong NN, Tu NHC, Kisiala A, Hoang XLT, and Thao NP. (2020). Role and regulation of cytokinins in plant response to drought stress. Plants 9: 422

Google Scholar: [Author Only](#) [Title Only](#) [Author and Title](#)

He Z, Wu J, Sun X, and Dai M. (2019). The maize clade APP2C phosphatases play critical roles in multiple abiotic stress responses. Int. J. Mol. Sci. 20: 3573

Google Scholar: [Author Only](#) [Title Only](#) [Author and Title](#)

Houbaert A, Zhang C, Tiwari M, Wang K, de Marcos Serrano A, Savatin DV, Urs MJ, Zhiponova MK, Gudesblat GE, Vanhoutte I, et al. (2018). POLAR-guided signalling complex assembly and localization drive asymmetric cell division. Nature 563: 574-578

Google Scholar: [Author Only](#) [Title Only](#) [Author and Title](#)

Huang Y, Wang X, Ge S, and Rao G-Y. (2015). Divergence and adaptive evolution of the gibberellin oxidase genes in plants. BMC Evol. Biol. 15: 207

Google Scholar: [Author Only](#) [Title Only](#) [Author and Title](#)

Hwang BG, Ryu J, and Lee SJ. (2016). Vulnerability of protoxylem and metaxylem vessels to embolisms and radial refilling in a vascular bundle of maize leaves. Front. Plant Sci. 7: 941

Google Scholar: [Author Only](#) [Title Only](#) [Author and Title](#)

Ikeda A, Ueguchi-Tanaka M, Sonoda Y, Kitano H, Koshioka M, Futsuhara Y, Matsuoka M, and Yamaguchi J. (2001). Slender rice, a constitutive gibberellin response mutant, is caused by a null mutation of the SLR1 gene, an ortholog of the height-regulating gene *GAI/RGA/RHT/D8*. Plant Cell 13: 999-1010

Google Scholar: [Author Only](#) [Title Only](#) [Author and Title](#)

Impens L, Jacobs TB, Nelissen H, Inzé D, and Pauwels L. (2022). Mini-Review: Transgenerational CRISPR/Cas9 gene editing in plants. Frontiers in Genome Editing 4: 825042

Google Scholar: [Author Only](#) [Title Only](#) [Author and Title](#)

Itoh H, Shimada A, Ueguchi-Tanaka M, Kamiya N, Hasegawa Y, Ashikari M, and Matsuoka M. (2005). Overexpression of a GRAS protein lacking the DELLA domain confers altered gibberellin responses in rice. Plant J. 44: 669-679

Google Scholar: [Author Only](#) [Title Only](#) [Author and Title](#)

Jacobs TB, Zhang N, Patel D, and Martin GB. (2017). Generation of a collection of mutant tomato lines using pooled CRISPR libraries. Plant Physiol. 174: 2023-2037

Google Scholar: [Author Only](#) [Title Only](#) [Author and Title](#)

Jacquier NMA, Gilles LM, Pyott DE, Martinant J-P, Rogowsky PM, and Widiez T. (2020). Puzzling out plant reproduction by haploid

induction for innovations in plant breeding. Nat. Plants 6: 610-619

Google Scholar: [Author Only](#) [Title Only](#) [Author and Title](#)

Jiao Y, Peluso P, Shi J, Liang T, Stitzer MC, Wang B, Campbell MS, Stein JC, Wei X, Chin C-S, et al. (2017). Improved maize reference genome with single-molecule technologies. Nature 546: 524-527

Google Scholar: [Author Only](#) [Title Only](#) [Author and Title](#)

Karimi M, Inzé D, Van Lijsebettens M, and Hilson P. (2013). Gateway vectors for transformation of cereals. Trends Plant Sci. 18: 1-4

Google Scholar: [Author Only](#) [Title Only](#) [Author and Title](#)

Knott GJ, and Doudna JA (2018). CRISPR-Cas guides the future of genetic engineering. Science 361: 866-869

Google Scholar: [Author Only](#) [Title Only](#) [Author and Title](#)

Koyama T, Sato F, and Ohme-Takagi M. (2017). Roles of miR319 and TCP transcription factors in leaf development. Plant Physiol. 175: 874-885

Google Scholar: [Author Only](#) [Title Only](#) [Author and Title](#)

Lampropoulos A, Sutikovic Z, Wenzl C, Maegele I, Lohmann JU, and Forner J. (2013). GreenGate - A novel, versatile, and efficient cloning system for plant transgenesis. PLoS ONE 8: e83043

Google Scholar: [Author Only](#) [Title Only](#) [Author and Title](#)

Lan J, and Qin G. (2020). The regulation of CIN-like TCP transcription factors. Int. J. Mol. Sci. 21: 4498

Google Scholar: [Author Only](#) [Title Only](#) [Author and Title](#)

Lawit SJ, Wych HM, Xu D, Kundu S, and Tomes DT. (2010). Maize DELLA Proteins dwarf plant8 and dwarf plant9 as Modulators of Plant Development. Plant and Cell Physiology 51: 1854-1868

Google Scholar: [Author Only](#) [Title Only](#) [Author and Title](#)

Li C, Hao M, Wang W, Wang H, Chen F, Chu W, Zhang B, Mei D, Cheng H, and Hu Q. (2018). An efficient CRISPR/Cas9 platform for rapidly generating simultaneous mutagenesis of multiple gene homoeologs in allotetraploid oilseed rape. Front. Plant Sci. 9: 442

Google Scholar: [Author Only](#) [Title Only](#) [Author and Title](#)

Li J, Wang Z, He G, Ma L, and Deng XW. (2020). CRISPR/Cas9-mediated disruption of TaNP1 genes results in complete male sterility in bread wheat. J. Genet. Genomics 47: 263-272

Google Scholar: [Author Only](#) [Title Only](#) [Author and Title](#)

Li N, and Li Y. (2016). Signaling pathways of seed size control in plants. Curr. Opin. Plant Biol. 33: 23-32

Google Scholar: [Author Only](#) [Title Only](#) [Author and Title](#)

Li W, Herrera-Estrella L, and Tran L-SP. (2016). The yin–yang of cytokinin homeostasis and drought acclimation/adaptation. Trends Plant Sci. 21: 548-550

Google Scholar: [Author Only](#) [Title Only](#) [Author and Title](#)

Li Y, Shan X, Jiang Z, Zhao L, and Jin F. (2021). Genome-wide identification and expression analysis of the GA2ox gene family in maize (*Zea mays* L.) under various abiotic stress conditions. Plant Physiol. Biochem. 166: 621-633

Google Scholar: [Author Only](#) [Title Only](#) [Author and Title](#)

Liebsch D, and Palatnik JF. (2020). MicroRNA miR396, GRF transcription factors and GIF co-regulators: a conserved plant growth regulatory module with potential for breeding and biotechnology. Curr. Opin. Plant Biol. 53: 31-42

Google Scholar: [Author Only](#) [Title Only](#) [Author and Title](#)

Liu H-J, Jian L, Xu J, Zhang Q, Zhang M, Jin M, Peng Y, Yan J, Han B, Liu J, et al. (2020). High-throughput CRISPR/Cas9 mutagenesis streamlines trait gene identification in maize. Plant Cell 32: 1397-1413

Google Scholar: [Author Only](#) [Title Only](#) [Author and Title](#)

Liu L, Gallagher J, Arevalo ED, Chen R, Skopelitis T, Wu Q, Bartlett M, and Jackson D. (2021). Enhancing grain-yield-related traits by CRISPR–Cas9 promoter editing of maize CLE genes. Nat. Plants 7: 287-294

Google Scholar: [Author Only](#) [Title Only](#) [Author and Title](#)

Long SP, Marshall-Colon A, and Zhu X-G. (2015). Meeting the global food demand of the future by engineering crop photosynthesis and yield potential. Cell 161: 56-66

Google Scholar: [Author Only](#) [Title Only](#) [Author and Title](#)

Lu Y, Ye X, Guo R, Huang J, Wang W, Tang J, Tan L, Zhu J-k, Chu C, and Qian Y. (2017). Genome-wide targeted mutagenesis in rice using the CRISPR/Cas9 system. Mol. Plant 10: 1242-1245

Google Scholar: [Author Only](#) [Title Only](#) [Author and Title](#)

McConnell JR, Emery J, Eshed Y, Bao N, Bowman J, and Barton MK. (2001). Role of PHABULOSA and PHAVOLUTA in determining radial patterning in shoots. Nature 411: 709-713

Google Scholar: [Author Only](#) [Title Only](#) [Author and Title](#)

Meng X, Yu H, Zhang Y, Zhuang F, Song X, Gao S, Gao C, and Li J. (2017). Construction of a genome-wide mutant library in rice using CRISPR/Cas9. *Mol. Plant* 10: 1238-1241

Google Scholar: [Author Only](#) [Title Only](#) [Author and Title](#)

Mickelbart MV, Hasegawa PM, and Bailey-Serres J. (2015). Genetic mechanisms of abiotic stress tolerance that translate to crop yield stability. *Nat. Rev. Genet.* 16: 237-251

Google Scholar: [Author Only](#) [Title Only](#) [Author and Title](#)

Miculan M, Nelissen H, Hassen MB, Marroni F, Inzé D, Pè ME, and Dell'Acqua M. (2021). A forward genetics approach integrating genome-wide association study and expression quantitative trait locus mapping to dissect leaf development in maize (*Zea mays*). *Plant J.* 107: 1056-1071

Google Scholar: [Author Only](#) [Title Only](#) [Author and Title](#)

Mills A, Allsman L, Leon S, and Rasmussen C. (2020). Using seed chipping to genotype maize kernels. *Bio-Protocol* 101: e3553

Google Scholar: [Author Only](#) [Title Only](#) [Author and Title](#)

Nelissen H, Rymen B, Jikumaru Y, Demuyneck K, Van Lijsebetsens M, Kamiya Y, Inzé D, and Beemster GTS. (2012). A local maximum in gibberellin levels regulates maize leaf growth by spatial control of cell division. *Curr. Biol.* 22: 1183-1187

Google Scholar: [Author Only](#) [Title Only](#) [Author and Title](#)

Nelissen H, Eeckhout D, Demuyneck K, Persiau G, Walton A, van Bel M, Vervoort M, Candaele J, De Block J, Aesaert S, et al. (2015). Dynamic changes in ANGUSTIFOLIA3 complex composition reveal a growth regulatory mechanism in the maize leaf. *Plant Cell* 27: 1605-1619

Google Scholar: [Author Only](#) [Title Only](#) [Author and Title](#)

Nuccio ML, Paul M, Bate NJ, Cohn J, and Cutler SR. (2018). Where are the drought tolerant crops? An assessment of more than two decades of plant biotechnology effort in crop improvement. *Plant Sci.* 273: 110-119

Google Scholar: [Author Only](#) [Title Only](#) [Author and Title](#)

Paul BK, Frelat R, Birnholz C, Ebong C, Gahigi A, Groot JCJ, Herrero M, Kagabo DM, Notenbaert A, Vanlauwe B, et al. (2018). Agricultural intensification scenarios, household food availability and greenhouse gas emissions in Rwanda: Ex-ante impacts and trade-offs. *Agric. Syst.* 163: 16-26

Google Scholar: [Author Only](#) [Title Only](#) [Author and Title](#)

Poland J, and Rutkoski J. (2016). Advances and challenges in genomic selection for disease resistance. *Annu. Rev. Phytopathol.* 54: 79-98

Google Scholar: [Author Only](#) [Title Only](#) [Author and Title](#)

Qin F, Kodaira K-S, Maruyama K, Mizoi J, Tran L-SP, Fujita Y, Morimoto K, Shinozaki K, and Yamaguchi-Shinozaki K. (2011). SPINDLY, a negative regulator of gibberellic acid signaling, is involved in the plant abiotic stress response. *Plant Physiol.* 157: 1900-1913

Google Scholar: [Author Only](#) [Title Only](#) [Author and Title](#)

Ramadan M, Alariqi M, Ma Y, Li Y, Liu Z, Zhang R, Jin S, Min L, and Zhang X. (2021). Efficient CRISPR/Cas9 mediated pooled-sgRNAs assembly accelerates targeting multiple genes related to male sterility in cotton. *Plant Methods* 17: 16

Google Scholar: [Author Only](#) [Title Only](#) [Author and Title](#)

Rasheed A, Hao Y, Xia X, Khan A, Xu Y, Varshney RK, and He Z. (2017). Crop breeding chips and genotyping platforms: progress, challenges, and perspectives. *Mol. Plant* 10: 1047-1064

Google Scholar: [Author Only](#) [Title Only](#) [Author and Title](#)

Rida S, Maafi O, López-Malvar A, Revilla P, Riache M, and Djemel A. (2021). Genetics of germination and seedling traits under drought stress in a MAGIC population of maize. *Plants* 10: 1786

Google Scholar: [Author Only](#) [Title Only](#) [Author and Title](#)

Rodríguez-Leal D, Lemmon ZH, Man J, Bartlett ME, and Lippman ZB. (2017). Engineering quantitative trait variation for crop improvement by genome editing. *Cell* 171: 470-480.e478

Google Scholar: [Author Only](#) [Title Only](#) [Author and Title](#)

Sarvepalli K, and Nath U. (2018). CIN-TCP transcription factors: transiting cell proliferation in plants. *IUBMB Life* 70: 718-731

Google Scholar: [Author Only](#) [Title Only](#) [Author and Title](#)

Schaumont D, Veeckman E, Van der Jeugt F, Haegeman A, Glabeke Sv, Bawin Y, Lukasiewicz J, Blugeon S, Barre P, de la O. Leyva-Pérez M, et al. (2022). Stack Mapping Anchor Points (SMAP): a versatile suite of tools for read-backed haplotyping. *bioRxiv* 2022.03.10.483555

Google Scholar: [Author Only](#) [Title Only](#) [Author and Title](#)

Simmons CR, Lafitte HR, Reimann KS, Brugièrè N, Roesler K, Albertsen MC, Greene TW, and Habben JE. (2021). Successes and insights of an industry biotech program to enhance maize agronomic traits. *Plant Sci.* 307: 110899

Google Scholar: [Author Only](#) [Title Only](#) [Author and Title](#)

Snowdon RJ, Wittkop B, Chen T-W, and Stahl A. (2021). Crop adaptation to climate change as a consequence of long-term breeding. *Theor. Appl. Genet.* 134: 1613-1623

Google Scholar: [Author Only](#) [Title Only](#) [Author and Title](#)

Sun X, Cahill J, Van Hautegeem T, Feys K, Whipple C, Novák O, Delbare S, Versteede C, Demuyneck K, De Block J, et al. (2017). Altered expression of maize PLASTOCHRON1 enhances biomass and seed yield by extending cell division duration. *Nat. Commun.* 8: 14752

Google Scholar: [Author Only](#) [Title Only](#) [Author and Title](#)

Teixeira FF, and Guimarães CT. (2021). Chapter 5 - Maize genetic resources and pre-breeding. In *Wild Germplasm for Genetic Improvement in Crop Plants*, M.T. Azhar and S.H. Wani, eds (London, United Kingdom: Academic Press, Elsevier), pp. 81-99

Google Scholar: [Author Only](#) [Title Only](#) [Author and Title](#)

Torella JP, Lienert F, Boehm CR, Chen J-H, Way JC, and Silver PA. (2014). Unique nucleotide sequence-guided assembly of repetitive DNA parts for synthetic biology applications. *Nat. Protoc.* 9: 2075-2089

Google Scholar: [Author Only](#) [Title Only](#) [Author and Title](#)

Vanhaeren H, Nam Y-J, De Milde L, Chae E, Storme V, Weigel D, Gonzalez N, and Inzé D. (2017). Forever young: the role of ubiquitin receptor DA1 and E3 ligase Big Brother in controlling leaf growth and development. *Plant Physiol.* 173: 1269-1282

Google Scholar: [Author Only](#) [Title Only](#) [Author and Title](#)

Vanhaeren H, Gonzalez N, Coppens F, De Milde L, Van Daele T, Vermeersch M, Eloy NB, Storme V, and Inzé D. (2014). Combining growth-promoting genes leads to positive epistasis in *Arabidopsis thaliana*. *eLife* 3: e02252

Google Scholar: [Author Only](#) [Title Only](#) [Author and Title](#)

Vats S, Kumawat S, Kumar V, Patil GB, Joshi T, Sonah H, Sharma TR, and Deshmukh R. (2019). Genome editing in plants: exploration of technological advancements and challenges. *Cells* 8: 1386

Google Scholar: [Author Only](#) [Title Only](#) [Author and Title](#)

Verbraeken L, Wuyts N, Mertens S, Cannoot B, Maleux K, Demuyneck K, De Block J, Merchie J, Dhondt S, Bonaventure G, et al. (2021). Drought affects the rate and duration of organ growth but not inter-organ growth coordination. *Plant Physiol.* 186: 1336-1353

Google Scholar: [Author Only](#) [Title Only](#) [Author and Title](#)

Vercruyse J, Baekelandt A, Gonzalez N, and Inzé D. (2020). Molecular networks regulating cell division during *Arabidopsis* leaf growth. *J. Exp. Bot.* 71: 2365-2378

Google Scholar: [Author Only](#) [Title Only](#) [Author and Title](#)

Voorend W, Nelissen H, Vanholme R, De Vliegher A, Van Breusegem F, Boerjan W, Roldán-Ruiz I, Muylle H, and Inzé D. (2016). Overexpression of GA20-OXIDASE1 impacts plant height, biomass allocation and saccharification efficiency in maize. *Plant Biotechnol. J.* 14: 997-1007

Google Scholar: [Author Only](#) [Title Only](#) [Author and Title](#)

Voss-Fels K, and Snowdon RJ. (2016). Understanding and utilizing crop genome diversity via high-resolution genotyping. *Plant Biotechnol. J.* 14: 1086-1094

Google Scholar: [Author Only](#) [Title Only](#) [Author and Title](#)

Wang B, Li N, Huang S, Hu J, Wang Q, Tang Y, Yang T, Asmutola P, Wang J, and Yu Q. (2021). Enhanced soluble sugar content in tomato fruit using CRISPR/Cas9-mediated SLINVINH1 and SIVPE5 gene editing. *PeerJ* 9: e12478

Google Scholar: [Author Only](#) [Title Only](#) [Author and Title](#)

Wang H-Q, Liu P, Zhang J-W, Zhao B, and Ren B-Z. (2020). Endogenous hormones inhibit differentiation of young ears in maize (*Zea mays* L.) under heat stress. *Front. Plant Sci.* 11: 533046

Google Scholar: [Author Only](#) [Title Only](#) [Author and Title](#)

Wang H, and Qin F. (2017). Genome-wide association study reveals natural variations contributing to drought resistance in crops. *Front. Plant Sci.* 8: 1110

Google Scholar: [Author Only](#) [Title Only](#) [Author and Title](#)

Winkler RG, and Freeling M. (1994). Physiological genetics of the dominant gibberellin-nonresponsive maize dwarfs, Dwarf8 and Dwarf9. *Planta* 193: 341-348

Google Scholar: [Author Only](#) [Title Only](#) [Author and Title](#)

Wu L, Zhang D, Xue M, Qian J, He Y, and Wang S. (2014). Overexpression of the maize GRF10, an endogenous truncated growth-regulating factor protein, leads to reduction in leaf size and plant height. *J. Integr. Plant Biol.* 56: 1053-1063

Google Scholar: [Author Only](#) [Title Only](#) [Author and Title](#)

Xiao Y, Tong H, Yang X, Xu S, Pan Q, Qiao F, Raihan MS, Luo Y, Liu H, Zhang X, et al. (2016). Genome-wide dissection of the maize ear genetic architecture using multiple populations. *New Phytol.* 210: 1095-1106

Google Scholar: [Author Only](#) [Title Only](#) [Author and Title](#)

Xing H-L, Dong L, Wang Z-P, Zhang H-Y, Han C-Y, Liu B, Wang X-C, and Chen Q-J. (2014). A CRISPR/Cas9 toolkit for multiplex genome editing in plants. BMC Plant Biol. 14: 327

Google Scholar: [Author Only](#) [Title Only](#) [Author and Title](#)

Zhang X, and Cai X. (2011). Climate change impacts on global agricultural land availability. Environ. Res. Lett. 6: 014014

Google Scholar: [Author Only](#) [Title Only](#) [Author and Title](#)

Zhang Y, Malzahn AA, Sretenovic S, and Qi Y. (2019). The emerging and uncultivated potential of CRISPR technology in plant science. Nat. Plants 5: 778-794

Google Scholar: [Author Only](#) [Title Only](#) [Author and Title](#)